Spring 2016

Fine-scale Topoclimate Modeling and Climatic Treeline Prediction of Great Basin Bristlecone Pine (Pinus longaeva) in the American Southwest

Jamis M. Bruening
Western Washington University, bruenij@students.wwu.edu

Fine-scale topoclimate modeling and climatic treeline prediction of Great Basin bristlecone pine (Pinus longaeva) in the American Southwest

By

Jamis M. Bruening

Accepted in Partial Completion
Of the Requirements for the Degree
Master of Science

Kathleen L. Kitto, Dean of the Graduate School

ADVISORY COMMITTEE

Chair, Dr. Andrew G. Bunn

Dr. Aquila Flower

Dr. David O. Wallin

MASTER'S THESIS

In presenting this thesis in partial fulfillment of the requirements for a master's degree at Western Washington University, I grant to Western Washington University the non-exclusive royalty-free right to archive, reproduce, distribute, and display the thesis in any and all forms, including electronic format, via any digital library mechanisms maintained by WWU.

I represent and warrant this is my original work, and does not infringe or violate any rights of others. I warrant that I have obtained written permissions from the owner of any third party copyrighted material included in these files.

I acknowledge that I retain ownership rights to the copyright of this work, including but not limited to the right to use all or part of this work in future works, such as articles or books.

Library users are granted permission for individual, research and non-commercial reproduction of this work for educational purposes only. Any further digital posting of this document requires specific permission from the author.

Any copying or publication of this thesis for commercial purposes, or for financial gain, is not allowed without my written permission.

Jamis M. Bruening
May 12th, 2016

Fine-scale topoclimate modeling and climatic treeline prediction of Great Basin bristlecone pine (Pinus longaeva) in the American Southwest

A Thesis
Presented to
The Faculty of
Western Washington University

In Partial Fulfillment
Of the Requirements for the Degree
Master of Science

By
Jamis M. Bruening
May, 2016

Abstract

Great Basin bristlecone pine (*Pinus longaeva*) and foxtail pine (*Pinus balfouriana*) are valuable paleoclimate resources due to the climatic sensitivity of their annually-resolved rings. Recent treeline research has shown that growing season temperatures limit tree growth at and just below the upper treeline. In the Great Basin, the presence of precisely dated remnant wood above modern treeline shows that this ecotone shifts at centennial timescales tracking long-term changes in climate; in some areas during the Holocene climatic optimum treeline was 100 meters higher than at present. This phenomena has motivated this analysis; regional treeline position models built exclusively from climate data may identify characteristics specific to Great Basin treelines and inform future physiological studies, and provide a measure of climate sensitivity specific to bristlecone and foxtail pine treelines. This study implements a topoclimatic analysis—using topographic position to explain patterns in surface temperatures across complex mountainous terrain—to model treeline position of three semi-arid bristlecone and/or foxtail pine treelines in the Great Basin as a function of topographically modified climate variables calculated from *in situ* measurements. Results indicate: (1) the treelines used in this study require a growing season length of between 143 - 152 days and average temperature ranging from 5.5 - 7.6 °C, (2) site-specific treeline position models may be improved through topoclimatic analysis—specifically the inclusion of an integrated measure of climate rather than a growing season isotherm measured in degrees, (3) treeline position in the Great Basin is likely out of equilibrium with the current climate indicating a potential shift in the primary growth-limiting factor at the highest elevations where trees are found.

Acknowledgments

I would like to thank my thesis advisor and committee chair Dr. Andy Bunn for his mentorship and guidance throughout this project, as well as my committee members for their time and effort in reviewing and improving this manuscript. Additionally, I'd like to acknowledge my fellow graduate student Tyler Tran for his involvement and assistance throughout; Stu Weiss for significant contribution throughout most phases of the analysis; Matthew Salzer for his bristlecone pine expertise, willing collaboration, and advice; and Jimmy Quenelle for his unparalleled field support.

Contents

List of Figures and Tables

List of Figures

List of Tables

1 Introduction

1.1 Climatic treeline formation

The treeline ecotone on a mountain is the region between closed montane forest and treeless alpine tundra. This boundary is not a distinct line, but rather a transition zone where the closed forest gives way to sparsely spaced stands and individual trees, eventually leading to a treeless landscape (Körner 2007, 2012). At regional and local scales factors such as water availability, slope, or substrate may influence treeline position, but at a global scale and across all tree species that form climatic treelines, *temperature* is thought to be the most influential factor (Wardle 1971; Jobbagy and Jackson 2000; Körner 2012). In mountainous terrain, local lapse rates determine the extent to which the atmosphere cools with increasing elevation. Consequently, trees within the treeline ecotone experience colder temperatures on average than trees growing farther downslope, inferring that at the highest elevations where trees are present, growth is primarily limited by low temperatures (Wardle 1971; Körner 2012). This is corroborated by significant relationships between annual ring widths from trees growing at or near treeline and growing season temperatures (LaMarche Jr 1973, 1974b; Salzer et al. 2009; Kipfmueller and Salzer 2010).

There is ample evidence supporting a low temperature limit theory for alpine treeline formation (Scuderi 1987; Jobbagy and Jackson 2000; Körner and Paulsen 2004; Körner 2012; Paulsen and Körner 2014). This theory states that (1) there are controls limiting biological processes that allow for tree growth at the highest elevations where trees are found, (2) these controls are physical (as temperatures approach 0 °C physiological activity ceases) and thus predictable and (3) are global in scale. A recent study published by Paulsen and Körner (2014) uses physiological parameters calculated from climate data to model the position of treeline globally. The authors define a threshold temperature (DTMIN) as the low temperature limit for physiological activity, and define the growing season as all days with an average daily temperature above the threshold value DTMIN. They use the threshold temperature (DTMIN) along with the length of the growing season (LGS) and the average daily temperature of all days within the growing season (seasonal mean temperature, SMT) to predict the position of

376 unique treelines around the globe. The model's best fit uses DTMIN = 0.9 °C, LGS = 94 days, and SMT = 6.4 °C, with a root mean square error between actual and predicted treeline position of 78 meters. The first of its kind, this study provides a framework for future treeline modeling efforts by targeting treeline physiology (physiological threshold DTMIN, growing season length LGS, growing season average temperature SMT).

This work and others (Scuderi 1987; Lloyd and Graumlich 1997; Salzer et al. 2013) provides evidence that treelines are valuable bioclimatic indicators, as changes in regional treeline positions have been shown to coincide with large-scale changes in climate. Changes in climatic conditions on the landscape affect the spatial location between the regions where tree physiological activity is possible and regions where it is not. This can be thought of as treeline position *potential*—the theoretical climatic boundary between areas where physiological activity is possible and areas where it is not possible. As climatic conditions change, this boundary shifts its position and tree demographic and/or mortality processes act to move treeline position until it stabilizes, reaching equilibrium with climatic conditions on the ground (Körner 2012). For example, a period of climate-cooling will force the theoretical *treeline position potential* downslope; trees now growing above this boundary are in locations where temperatures are too cold for physiological activity, and over time will die out. Conversely, a period of climate-warming will force this boundary upslope; over time demographic process of seedling recruitment and establishment move actual treeline position upward as trees start to establish in the newly-suitable region above the old treeline position. The demographic and mortality processes that actually shift the treeline position on the landscape are known to act on much longer timescales than the changing climatic conditions that initiate the shift in treeline position, however a comprehensive review of tree demography and mortality at treeline is outside the scope of this analysis (Körner 2012). Broadly speaking, both upslope and downslope changes in treeline position lag behind large scale changes in climate by at least 50 - 100 years (Scuderi 1987; Körner 2012). Treeline dynamics studies, especially estimates of changes in treeline position through extensive sampling of treeline trees and remnant wood above treeline provide climatic insights backwards in time that far surpass the length of the instrumental record (Salzer et al. 2013). Such insights are only possible through a comprehensive under-

standing of the physiology of treeline formation, as well as the interaction between treeline dynamics and climate—both of which have motivated this analysis.

1.2 Great Basin treelines

In the American Southwest, Great Basin bristlecone pine (*Pinus longaeva*, D.K. Bailey) and foxtail pine (*Pinus balfournaia*, Grev. & Balf.) grow at the highest elevations where trees are found in various mountain ranges. These closely related five-needle pine species are extremely long lived, and display similar climate-growth responses. Specific individuals have been known to reach 5,000 years (Currey 1965). Various studies have used both bristecone and foxtail pine chronologies in unison for paleoclimatic inference (Scuderi 1987; Lloyd and Graumlich 1997). Their natural habitat is particularly harsh and arid; cold temperatures persist for much of the year and the growing season is extremely dry, as most precipitation falls as snow during the winter months (LaMarche Jr 1973; Scuderi 1987; Salzer et al. 2009).

Throughout the 20th and 21st centuries, dendroclimatological bristlecone and foxtail pine research has focused on identifying the main limiting factors throughout the species' range. These species are treeline-forming, and are well adapted to the arid subalpine environments in the Great Basin. At the upper reaches of both species, the closed forest ecotone gives way to sparsely spaced stands and individual trees, eventually transitioning to a treeless landscape. This boundary is the upper climatic treeline, and many studies have shown tree growth there is most limited by growing season temperatures (LaMarche Jr 1973; LaMarche Jr and Stockton 1974; Salzer et al. 2009). At the lower boundary of their distribution, the forest composition transitions to more ecosystems requiring longer growing-seasons. In the southeast Sierra Nevada, foxtail pine forests transition to lodge pole pine (*Pinus contorta*) dominated ecosystems. Farther northeast in the White Mountains and other smaller mountain chains endemic to Great Basin bristlecone pine, the forests transition to mixed ecosystems composed of piñon pine (*Pinus cembroides*), juniper (*Juniperus*), and limber pine (*Pinus flexilis*). It is well documented that growth near the lower boundary of bristlecone and foxtail is predominately controlled by precipitation and soil moisture availability (LaMarche Jr 1974a; Hughes and Funkhouser 2003). Combining evidence of these species growth-limitation at the

upper and lower treelines suggests the main limiting factor of tree growth operates on a gradient, changing from moisture limitation at the lower treeline to temperature limitation at the upper treeline (Kipfmueller and Salzer 2010; Salzer et al. 2014). For clarity, the term 'treeline' henceforth refers to the upper treeline, as this boundary is the main subject of this analysis. Discussion of the lower, drought-limited treeline will clearly specified as such.

Recent studies by Salzer and colleagues (Bunn et al. 2011; Salzer et al. 2009, 2013, 2014) have focused on determining the extent to which temperature and/or precipitation influences individual trees' growth based on the proximity to upper treeline. Specifically, their work is aimed at determining where, in relation to treeline, individuals switch from being moisture sensitive to temperature sensitive, and explaining the mechanisms that cause this shift. An underlying assumption of dendrochronology is that trees located 'near' one another (at the same site) are limited by the same environmental factor (i.e. temperature or moisture availability). By building a chronology with many samples from a single location, values of that site's limiting factor can be reconstructed via correlations with ring width measurements (Fritts 1976). Recent work by Bunn et al. (2011) shows that trees growing only tens of meters apart may be limited by different environmental factors, based on differences in topography between such trees. They suggest 'topographically modified chronologies' may be more accurate than traditional methods for paleoclimate reconstructions, by isolating trees limited by the same environmental factor through a topographic analysis. Further work by Salzer et al. (2014) builds on these findings through analysis of near-treeline chronologies from different aspects. Their findings corroborate Bunn et al. (2011) as growth patterns from similar elevations observed on different aspects at the same site were shown to diverge. Additionally, there seems to exist a "climate response threshold, approximately 60-80 vertical meters below treeline, above which trees have shown a positive growth-response to temperature and below which they do not" (Salzer et al. 2014). Both studies propose that differences in topography and even small changes in elevation may be enough to significantly alter the growth response between trees growing in close proximity, and suggest further work to fully investigate these findings.

1.3 Topoclimate

The work of Bunn et al. (2011) and Salzer et al. (2014) provide evidence of topographic influences on tree growth. In the past several decades significant research has been dedicated to identifying and quantifying the influences of mountainous topography on temperatures, and subsequently on biological systems (Weiss et al. 1988; Lookingbill and Urban 2003; Ashcroft et al. 2009; Dobrowski et al. 2009; Geiger et al. 2009; Dobrowski 2011; Adams et al. 2014). Dobrowski et al. (2009) provides an excellent discussion of the influences of topography on climate, explanation of the term *topoclimate*, and review of relevant literature. Topoclimatic modeling attempts to explain variations in temperature due to local topographic features, independent of changes in elevation (Lookingbill and Urban 2003; Dobrowski et al. 2009). Taken in conjunction with recent bristlecone pine research regarding temperature limitation at the highest elevations (LaMarche Jr 1973; Salzer et al. 2009) and Körner's and other's work investigating climate-limited treeline position (Wardle 1971; Jobbagy and Jackson 2000; Körner and Paulsen 2004; Körner 2012; Paulsen and Körner 2014), there is reason to believe that a treeline position model that accounts for topographic influences on temperatures may yield new insights into regional and smaller scale controls on treeline position (Weiss et al. 2015).

1.4 Objectives

Paulsen and Körner's (2014) global model (TREELIM) identifies three parameters (physiological threshold DTMIN, growing season length LGS, growing season average temperature SMT) that constrain treeline position globally, including many different treeline-forming species throughout diverse climate zones. My analysis seeks to compare the results of TREELIM to a site-and-species-specific treeline analysis of three semi-arid Great Basin treelines. I use a down-scaled approach, adapting methodology from Paulsen and Körner (2014), to compare the characteristics of treelines formed by bristlecone and foxtail pines to the global model. My work attempts to better understand and quantify the physiological limits of Great Basin treeline-forming species due to their immense value as a climatic proxy. Inspired by recent

work regarding the low temperature theory for treeline formation, I employ current knowledge of topoclimatology and bristlecone pine growth-limitation to predict treeline position as a function of climate.

Explicitly stated, my objectives are to:

1. Identify complex topographic influences on surface temperatures in diverse mountainous terrain, specifically identifying differences between lapse-rate dependent cooling and other trends independent of elevation;

2. Model the position of three climate-limited treelines in the Great Basin as a function of topographically modified climate variables known to influence tree growth at those locations;

3. Compare the characteristics of the Great Basin treelines to other treelines globally, seeking to quantify physiological limits of tree growth at treeline in the Great Basin.

The first part of this analysis involves topoclimatic modeling of *in situ* temperature measurements, using regression models to predict monthly-resolved climate variables across the landscape as a function of elevation and topography. I use these outputs to calculate treeline variables developed by Paulsen and Körner (2014), and build classification models predicting treeline position as a function of topoclimate and treeline-specific variables. This fine-scale approach (10 meter resolution) allows for a rigorous analysis of the topographic controls on mountain climates at a height of one meter, and provides evidence supporting the theory of climatic treeline formation. Additionally, this work provides insights into bristlecone pine physiology and treeline dynamics, both of which are extremely important given the value of bristlecone pine chronologies to paleoclimatic studies. To my knowledge this methodology is novel, as other treeline analyses operate at coarser resolutions (Jobbagy and Jackson 2000; Paulsen and Körner 2014; Weiss et al. 2015).

2 Methods

2.1 Site Selection

Treeline sites in the Great Basin are typically remote areas not easily accessible by vehicle. Accordingly, site selection was influenced by ease of access for sampling, as well as the presence of an obvious climate-limited treeline and ample topographic heterogeneity to ensure enough leverage in the models. I chose four high-elevation sites at the upper range of both bristlecone and foxtail pine, three of which were used by Salzer et al. (2013) for the presence of a climatic treeline and numerous pieces of remnant wood and standing dead snags above current treeline position: (1) Sheep Mountain, White Mountains, CA (SHP, 37.52°N. lat., 118.20°W. long., treeline position roughly 3500 m.a.s.l.), (2) Mount Washington, Snake Mountain Range, NV (MWA, 38.91°N. lat., 114.31°W. long., treeline position roughly 3400 m.a.s.l.), and (3) Pearl Peak, Ruby Mountain Range, NV (PRL, 40.23°N. lat., 115.54°W. long., maximum elevation roughly 3300 m.a.s.l.). I included a fourth site, Chicken Spring Lake, Sierra Nevadas, CA (CSL, 36.46°N. lat., 118.23°W. long., treeline position roughly 3600 m.a.s.l.), which has a distinct and continuous climatic treeline formed by foxtail pine, also with existing remnants and dead snags located above treeline. Accessible treeline sites with extensive remnant and standing dead snags above treeline are relatively rare, and due to documented similarities between foxtail and bristlecone pines, I decided CSL was a valuable addition to this analysis.

PRL is the only site chosen without the presence of an obvious climatic treeline; there are several areas that may have climate limited treeline, yet across the entire site the treeline is not fully formed and the alpine and treeline ecotones are not present in a comparable fashion to the alpine and treeline ecotones at the other sites. Despite the lack of a distinct treeline, PRL is still an excellent location for the temperature modeling portion of this analysis due to the unique combination of topographic features found there, as discussed later. However, it has been excluded from the classification modeling portion of this analysis.

MWA, CSL, and SHP have obvious climatic treelines present on the landscape, yet the characteristics of the treeline at SHP are slightly different than at MWA or CSL. The White Mountains are named for the bright white color of the dolomite substrate commonly found

there. This substrate is an ideal habitat for Great Basin bristlecone pine, and for the most part the climatic treeline at this site is found growing in areas with exposed dolomite substrate. Other obvious treelines are evident at this location, but may be influenced in some part by the substrate composition and thus have been excluded form this analysis. The climatic treeline at SHP used in this analysis is limited to areas with exposed dolomite—a distance of about 8 kilometers. While this fact does not preclude SHP from the treeline prediction modeling, the unique nature of this site must be included in the discussion as it sets this site apart slightly from MWA and CSL.

2.2 Sensor Placement

The topoclimate modeling portion of this analysis involved recording temperatures to build predictive temperature models from values of the local topography. I used thermochron iButton sensors manufactured by Maxim Integrated, San Jose CA model DS1922L-F5, with an accuracy of ± 0.5 °C. At each site, I used 50 sensors to record hourly temperatures over the course of one year; from September 2013 - September 2014 at MWA and PRL, and from September 2014 - 2015 at SHP and CSL. The sensors were mounted at a height of one meter in living trees, secured inside white PVC t-joints to block direct sunlight from overheating the sensors' metal exterior. I worked with my thesis adviser (Andy Bunn) and another committee member (Stu Weiss) to develop a network of sensor placements at each site to maximize topographic heterogeneity between individual placements (in almost all cases, sensors were mounted no more than 100m from neighboring sensors). In mountainous environments topographic position has a significant influence on 1 meter temperatures (Lookingbill and Urban 2003; Fridley 2009). Local lapse rates remain a dominant factor influencing climate, however topography-driven phenomena such as cold air drainage and differences in aspect and solar radiation loads also have significant effects on daily temperatures, and contribute significantly to a location's climate (Geiger et al. 2009). Bunn et al. (2011) showed tree growth is influenced by the topography at that location, suggesting topography influences mountain climate at

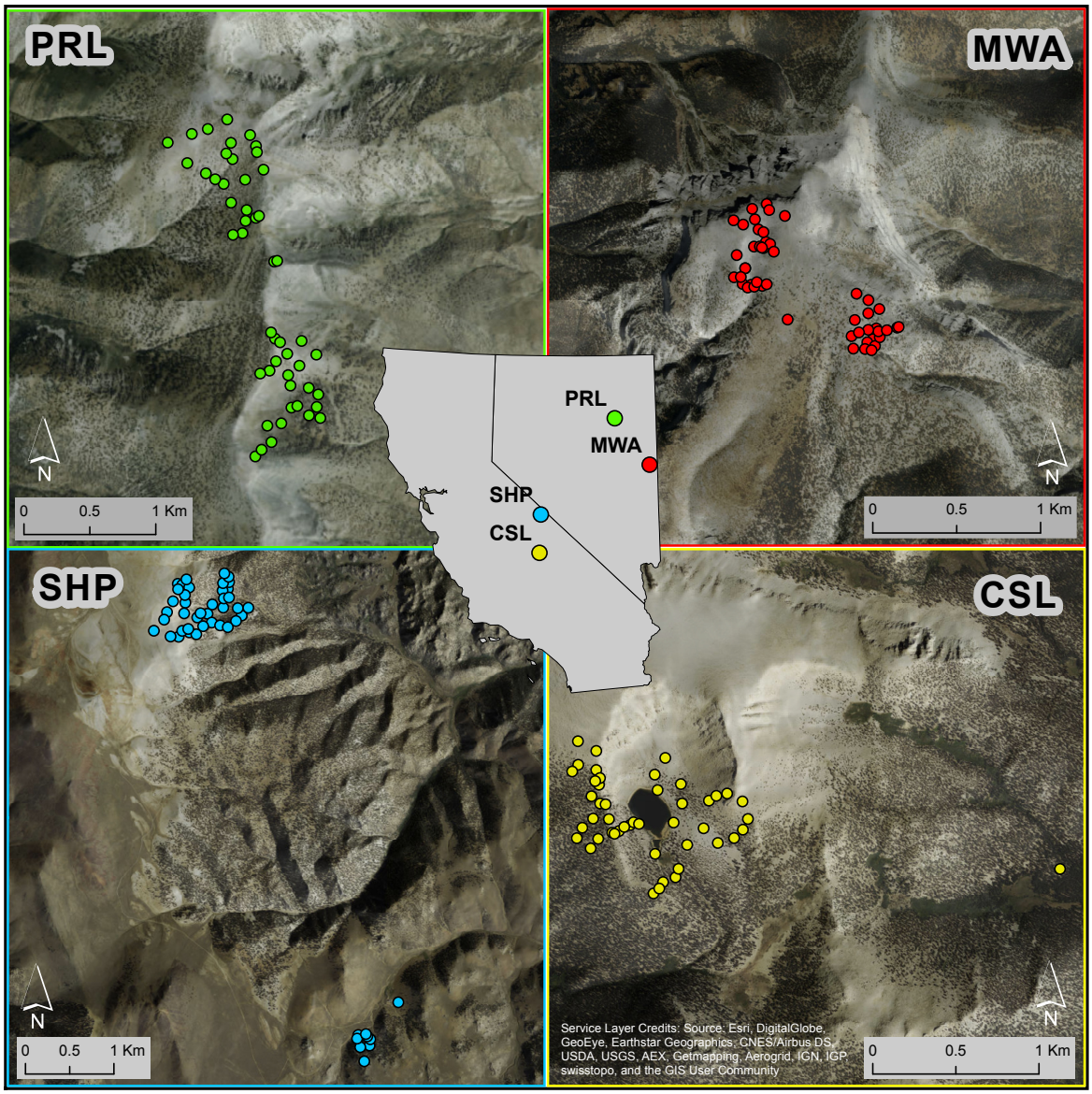

Figure 1: iButton locations with a satellite imagery basemap to show proximity to treeline

scales as small as tens of meters. At these sites topography varies considerably on the scale of tens of meters, dictating a sensor network dense enough to capture the fine-scale topographic effects on climate. Accordingly, developing the network of sensor placements was a balance between trying to cover a large area with a representative sampling of topographic heterogeneity for each site, while minimizing the distance between placements to allow for accurate interpolation. Additionally, I placed one or two sensors were placed farther away and at lower

elevations than the rest, to aid in local lapse rate calculations.

2.3 Data Preprocessing

Before modeling, the data recorded by the sensors required significant quality control and preprocessing measures. The primary objective of this approach (using individual sensors to record temperatures at 50 unique locations with diverse topographic features) was to capture the effects of topography on climate in mountainous regions. Thus the raw recorded values were of less direct importance than the relative differences between sensors, caused by differences in topographic position. One of the shortcomings of this approach is that I use information associated with single year's *weather* at a site to draw inferences about its *climate*. A location's climate is a multi-year average of the weather conditions experienced there—weather conditions from a single year rarely match perfectly with the climate of that location. Accordingly, the quality control and processing methods I developed attempt to improve the inference gained from the models by correcting for weather anomalies during the period of data collection to better represent the climate at these sites, and *do not* alter the information about topographic effects on surface temperature captured by each sensor network.

Figure 2 outlines the methods I used for data processing to correct various anomalies at hourly and monthly scales and account for missing data: (1) I identified and corrected anomalous hourly values due to direct sunlight striking individual sensors; (2) I modeled missing data at the beginning and end of each deployment period from stable relationships between the sensors recorded values and data from the Parameter-elevation Regressions on Independent Slopes Model (PRISM); (3) to better represent the annual climate at each site, I adjusted the aggregated monthly variables by a delta factor representing the difference in each monthly temperature between the year of sensor deployment (October 2013 - September 2014 for MWA and PRL, and October 2014 - September 2015 for CSL and SHP) and the average monthly temperature from 1895-2015 calculated from monthly PRISM data (PRISM 2004); and (4) I adjusted all the data 1.5 °C, representing a conservative estimate of warming in the Great Basin between the period when present treeline position was established (estimated to

be 1328 A.D. by Salzer et al. (2013)) and present conditions. Explanation of the justification for and specific methodology of each adjustment technique is explained in the following sub-sections.

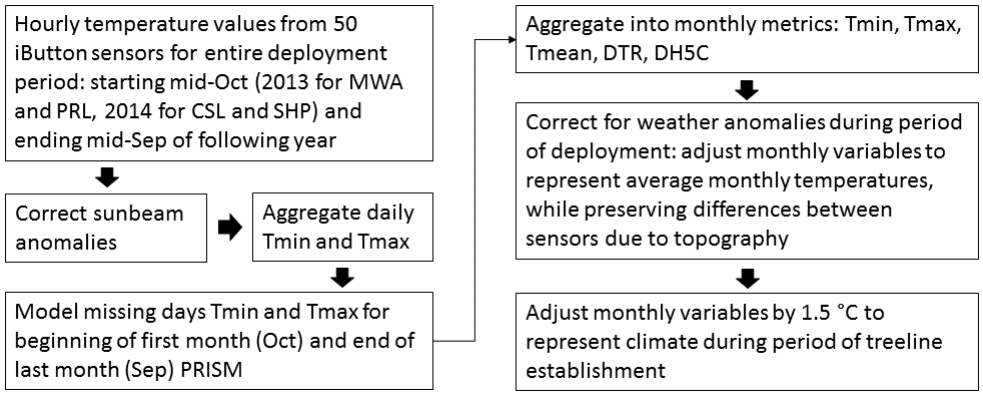

Figure 2: Schematic outline of hourly iButton data processing workflow. This process was implemented at each site

2.3.1 Sunbeam Interpolation

There was evidence of direct sunlight striking individual sensors despite being covered by radiation shields. To identify those affected and at what times, I averaged the data by hour from May 01 - August 31, and plotted the average daily temperature profile for each sensor. Hours specific sensors were in direct sunlight were evident by distinct spikes in the 24-hour profile, occurring primarily in the early morning or late afternoon due to low sun angle. For consistency I developed a program to identify and mark specific hours when a sensor's average hourly temperature was greater 0.75 °C greater than the hour before and after it. I disregarded the anomalous values and used cubic spline interpolation to calculate realistic temperatures values for the affected time period. The number of sensors that required correction at each were: 13 at MWA, 12 and PRL, 17 at CSL, and at 13 SHP.

2.3.2 Modeling Missing Data

The storage capacity of the sensors was not enough to record a full year of hourly values. I was missing data from the first several weeks of deployment for each site, as well as the last several

weeks of the month during which the sensors were collected (For example, the MWA sensors were collected on September 15th 2014, and to calculate monthly variables for September 2014, I needed values for the remaining two weeks in the month.). To solve this problem, I aggregated the hourly sensor data into daily minimum and maximum values, by calculating the minimum and maximum values in each 24-hour period. I then calculated linear models between each sensor's daily value and that site's PRISM value (PRISM 2004), and for each missing day predicted the sensor's value from the model. This method relies on a consistent relationship between each sensor's daily values and the PRISM value for that site, which was confirmed through graphical analysis. See appendix I for more information.

2.3.3 Data Aggregation

From the hourly data, five monthly climate variables were calculated: monthly average minimum and maximum temperatures (Tmin, Tmax) represent the average daily minimums and maximums within each month; monthly average temperatures (Tmean) were calculated by averaging all hourly values within each month; and diurnal temperature ranges (DTR) were calculated from the difference between the daily minimums and maximums and averaged into monthly values. The final metric—degree hours above 5 °C (DH5C)—is a measure of the number of hours temperatures were above 5 °C. Degree hour calculations are integrated measures of temperature by hour, above or below a defined threshold value. For example if the temperatures for three consecutive hours are measured at 10 °C, 12 °C, and 15 °C, the total growing degree hours above 5 °C for the three hour time span would be equal to 22 °C (10 °C - 5 °C + 12 °C - 5 °C + 15 °C - 5 °C = 22 °C). DH5C could not be calculated for the entirety of September or October, due to the lack of hourly data during these months due to the storage capacity issue. Thus September and October DH5C values are truncated and have been excluded as predictive variables in this analysis. The four final data sets (one for each site), contain the five, monthly-resolved climate variables for 50 unique locations at each site.

2.3.4 Weather vs. Climate Correction

Having recorded a single year of temperature values at each site, the data were not necessarily representative of the climate (multi-year average of temperatures) at each site. The value of recording temperatures at 50 unique locations comes from the ability to model the recorded

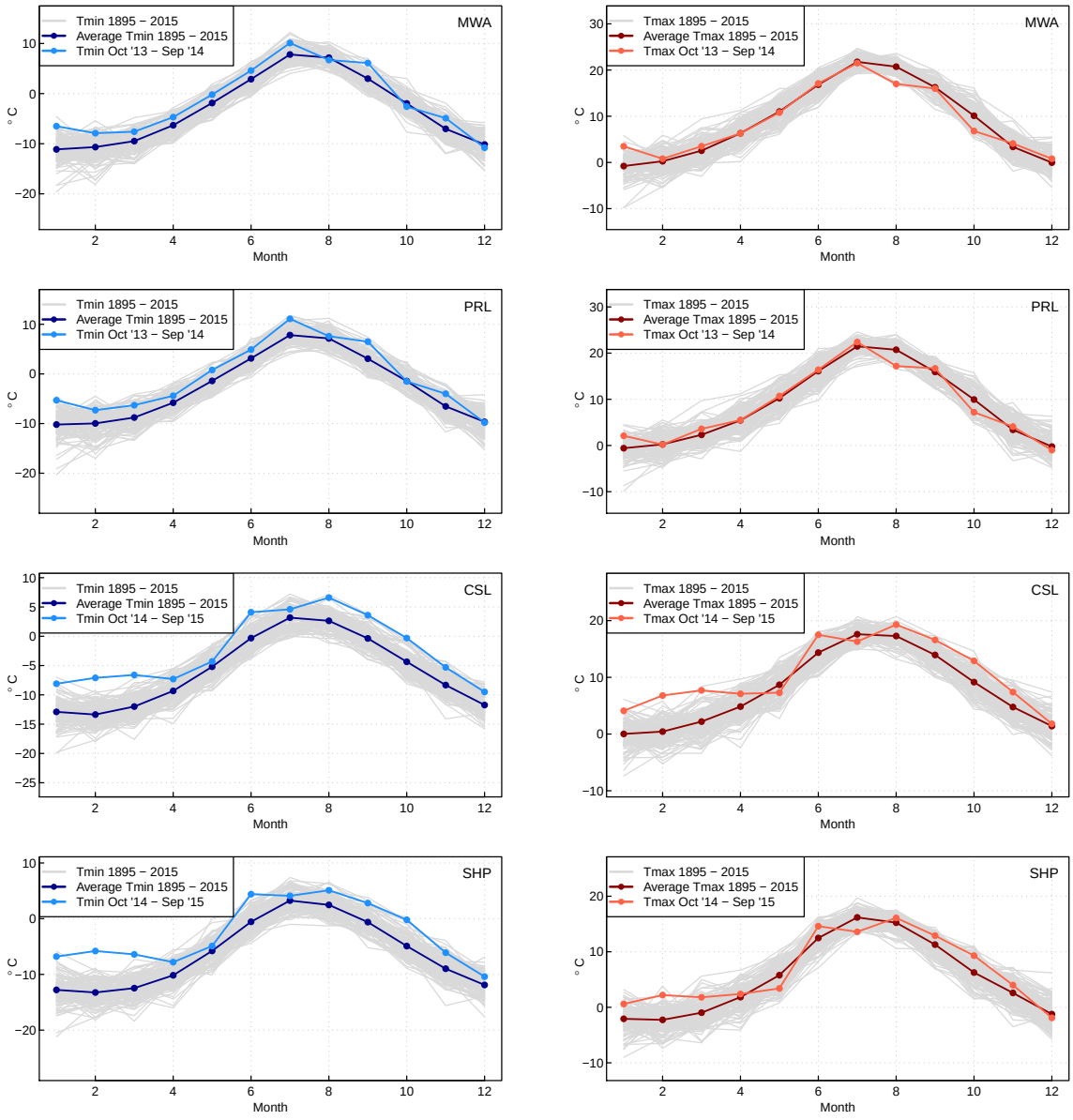

Figure 3: Minimum (light blue) and maximum (orange) temperature during the period of iButton deployment at each site plotted against a 120 climate normal of minimum (dark blue) and maximum temperatures (dark orange)

values as a function of the local topography. To predict treeline position as a function of average growing season climate, temperature values representative of the *climate* at a location must be used, as treeline position shifts occur over tens or even hundreds of years, and have been linked to climate variables rather than the weather during any specific year (Körner 2012; Paulsen and Körner 2014; Millar et al. 2015). This is especially critical to identifying the physiological limits of treeline-forming species—results obtained from models using an anomalous year's weather would be unrepresentative of the actual limits that are a function of climate, rather than weather. Henceforth, when used to discuss variables calculated from the iButton data, the term *climate* refers to a multi-year average of temperature values, while discussion of temperatures or specific weather conditions will be explicitly denoted.

Figure 3 shows several months temperatures during October 2013 - September 2015 were anomalous when compared to the average monthly temperatures calculated from the entire instrumental record. At each site, I used monthly PRISM temperatures from the entire instrumental record (1895 - 2015) to calculate a 120 year monthly climate normal, and calculated a delta factor between the climate normal and the monthly PRISM temperatures during the period of data collection. I subtracted the monthly anomalies from the aggregated monthly variables, adjusting the values to better represent the climate at each site, while preserving the differences between individual sensors' values. The DH5C variable requires hourly data, rather than monthly data, so a simple subtraction was not sufficient to correct the monthly anomalies. I used the original, raw data to calculate linear models for each month's DH5C values as a function that Tmin and Tmax data from that month, and used the anomaly-adjusted Tmin and Tmax to calculate an adjusted DH5C values representative of each sites' climate, using the coefficients and intercepts from each linear model.

2.3.5 Paleoclimate Adjustment

To calculate the physiological limits of bristlecone and foxtail pine growth at treeline, I needed to identify the period in time when the current treeline positions were formed. Treeline position lags changes in climatic conditions, so treeline position today may be lower than its actual full potential height due to recent warming in the past several centuries. This is evidenced

by recent studies showing new recruitment patterns in bristlecone pine forests above current treeline at multiple sites in the Great Basin (Salzer et al. 2009; Millar et al. 2015). Thus, using today's climate to predict treeline positions that were influenced by a cooler climate hundreds of years ago would yield spurious conclusions about the physiological growth-limits at treeline. Through extensive sampling of living trees at treeline and of remnant wood above treeline, Salzer et al. (2013) conclude that (1) the current treeline positions at MWA and SHP were formed in the early 1300s A.D., and (2) have not shifted since. The authors provide a Great Basin climate reconstruction of temperature anomalies relative to the period of A.D. 1000-1990 from bristlecone pine chronologies near treeline at MWA, PRL, and SHP. Their data show an approximate warming of 1.4 °C in the Great Basin since the approximate date of treeline position stabilization, around 1328 A.D.. Using Salzer et al.'s (2013) data, I obtained a more exact value of this warming by calculating the difference between the temperature anomaly the authors reported for the period when the treelines formed their current position, and the temperature anomaly for the current climate. To find the temperature anomaly when Great Basin treelines formed their current position, I calculated a 100-year average of the reconstruction values centered on 1328 A.D., as treeline position requires multiple years to fully stabilize its position (Körner 2012). To find the anomaly for today's climate, I used the data after 1900 A.D. to calculate a linear model estimate the value of the reconstruction in 2014 when my sensors were recording temperatures, as the latest year presented in the reconstruction was 2003. The difference between these values was 1.5 °C, and I subtracted this value from the aggregated climate variables. The newly adjusted climate variables represent the climate when the current treeline positions in the Great Basin stabilized, and were the values used in the topoclimate models.

After the four quality control and processing techniques were implemented, the final data set for each site consisted of five monthly resolved climate variables—Tmin, Tmean, Tmax, DTR, and DH5C—adjusted to represent the monthly climate during the early 1300s A.D., when treelines are thought to have established in the Great Basin.

2.4 Topoclimate Modeling

2.4.1 Topographic Data

In mountainous environments, topography has a significant effect on local climates, even when elevation remains constant, so a simple lapse rate calculation was not sufficient to predict the climate variables across the landscape (Dobrowski 2011). Thus, I generated a suite of topographic variables thought to influence mountainous climates, to use as the predictive variables in each model. All predictive variables were calculated from a 1/3 arc second (10 m) Digital Elevation Model (DEM) obtained from the United States Geological Survey, yielding all predictive variables at 10m resolution. Raster surfaces representing slope, aspect, and daily solar radiation loads from the 21st of each month during the growing season (April - October) were calculated directly from the DEM using the ArcMap Spatial Analyst toolbox (ESRI 2012). Two continuous aspect derivatives, eastness and southness, were developed to eliminate the discontinuity of aspect values. Eastness and southness indices ranged from 1 (for vertical surfaces facing directly east and south, respectively) to -1 (for vertical surfaces facing directly west and north, respectfully). In conjunction these variables represent the exact aspect of a specific location, and can be used in modeling efforts more effectively than a measure of aspect in degrees.

A set of topographic position indices ($\mathrm{TPI_{x,y,r}}$) representing the difference between the elevation at specific point and the average elevation of a larger area surrounding that point were calculated using the formula:

$$TPI_{\mathrm{x,y,r}} = E_{\mathrm{x,y}} / \bar{E}_{\mathrm{x,y,r}}$$

in which $TPI_{\mathrm{x,y,r}}$ is the topographic position value of specified radius r at a specific location (x, y); $E_{\mathrm{x,y}}$ is the elevation at that specific point; and $\bar{E}_{\mathrm{r,x,y}}$ is the average elevation within a circle of radius r centered on point (x, y) (Weiss 2001). Values of $TPI_{\mathrm{x,y,r}}$ were generated for r = 25m, 50m, 100m, 200m, 300m, 400m, 500m, and 1000m.

Another topographic index representing a location's topographic convergence (TCI, also known as the topographic wetness index or TWI) was used as an estimate of cold-air pooling,

and calculated using the following formula:

$$TCI_{\mathrm{x,y}} = \ln(\alpha_{\mathrm{x,y}} / \tan \beta_{\mathrm{x,y}})$$

in which $TCI_{\mathrm{x,y}}$ is the value of topographic convergence at location (x, y); $\alpha_{\mathrm{x,y}}$ is the up slope contributing flow area calculated using the ArcMap Spatial Analyst toolbox (ESRI 2012); and $\beta_{\mathrm{x,y}}$ is the slope at location (x, y). Higher values of TCI represent converging topography—such as concave slopes or drainages—and potentially wetter areas as converging topography leads to surface runoff accumulation; lower values represent represent diverging topography—such as a ridge line or summit—that are typically drier areas with less runoff accumulation.

2.4.2 Model Construction

Many of my topographic predictor variables were correlated with eachother, and thus I used a LASSO regression from the R package 'caret' (Kuhn 2015) to model each monthly climate variable. This approach allows for highly correlated predictor variables, and seeks to minimize the influence of variables less important for prediction, and identifies only the most predictive variables in each model. I used a k-fold cross validation technique with $k = 10$ and 10 repeats per fold to guard against over fitting. The models were then used to predict the climate variables across the entire study site above 3000 meters at 10 meter resolution. The resultant topoclimatic data set consists of 60 maps, representing the influences of topography on each predicted variable.

2.5 Classification Modeling

I used climate data from the topoclimate models to build classification models predicting climatic treeline position as a function of temperature. PRL did not have enough of an established climatic treeline to enable modeling, so the analysis in the following section was only performed at MWA, SHP, and CSL. I used the 'rpart' package in R to build the classification models (Therneau et al. 2015). This software package is a variation of the methods presented

in the CART book written by Breiman et al. (1984). This approach was used over other methods (such as random forest modeling) because it yields a single classification tree, rather than a forest of trees and classification probabilities. This single tree is extremely useful, in that it displays the threshold values used in the model, allowing for insights to be drawn regarding a physiological threshold between each ecotone. The predictive variables used were the outputs of the topoclimate models (Tmin, Tmean, Tmax, DTR, and DH5C at monthly resolution) as well as two treeline variables (length of the growing season LGS and average temperautre throughout it SMT, explained in section 1.1) used by Paulsen and Körner (2014) in their global treeline model. I calculated raster layers of these variables from the monthly Tmean topoclimate predictions using the same methodology as Paulsen and Körner (2014), assuming their best fit value of DTMIN (0.9 °C). I used cubic splines to interpolate between the monthly Tmean temperatures and calculate daily Tmean values, summing all days with an average temperature above 0.9 °C to calculate the length of the growing season (LGS), and averaging the temperature of all days within the growing season to find the mean temperature throughout it (SMT). These calculations were performed spatially, yielding maps representing values of each variable for the same extent as the topoclimate layers.

2.5.1 Training Ecotones

I built classification models to predict three different treeline-related ecotones—subalpine, treeline, and alpine (see figure 4)—using the topoclimate predictions as predictive variables. The ecotone boundaries were delineated in Google Earth and follow accepted definitions and conventions set by Körner (2007).

The treeline ecotone is a transitional boundary between the uppermost edge of closed montane forest and the treeless landscape found at the highest elevations at these sites. To define the areas at each site within the treeline ecotone required a multi-step process. I used satellite imagery in Google Earth to digitize a line on the landscape that best represents the treeline ecotone (represented by the letter C in figure 4). This was a somewhat subjective process, relying on the accepted definitions of this ecotone within the relevant literature (Körner 2007, 2012), as well as my experience on the ground at these sites and my understanding of where

the ecotone boundaries fall on the landscape. In general the line tracked the upper-most reaches where mature trees were seen to be present, while maintaining a relatively smooth, straight path. At the landscape scale, the width of the treeline ecotone measured parallel to the mountain slope depends on the slope at each locaton along it (see figure figure 5). Thus to ensure that my digitized boundaries captured the entire width of the 'true' treeline ecotone I set a conservative buffer on either side of the line and defined the area within the upslope and downslope buffers as the treeline ecotone (the yellow shaded region in figure 4). The upslope buffer was set a distance sufficiently far uphill from the line (50 horizontal meters, marked by the letter D in figure 4) to ensure it surpassed the 'true' boundary between the alpine and treeline ecotones. The downslope buffer was set to a larger distance (100 horizontal meters, marked by the letter B in figure 4) to ensure that no part of the treeline ecotone was included in the subalpine ecotone. The buffers on either side of the treeline (letter C in figure 4) likely stretch beyond true boarders of the treeline ecotone in some places, as the slope ultimately dictates the width of the ecotone. Thus, when extracting climate information for this ecotone for the classification models, I only used points along the digitized *line* (letter C in figure 4) to exclude any data representing the other ecotones from being included in the treeline ecotone. With the upper and lower boundaries of the treeline ecotone set (represented by letters D and C respectively in figure 4), I was then able to define the areas of the subalpine and alpine ecotones; both ecotones were defined to be 150 horizontal meters wide for consistency with the treeline ecotone, and extent downslope and upslope (respectfully) from their boarder with the treeline ecotone (in figure 4, the green shaded area bounded by letters A and B represents the subalpine ecotone, while the blue shaded region bounded by letters D and E represents the alpine ecotone). All distances were measured horizontally, so the width of each ecotone measured parallel to the slope may vary slightly, although these effects average out across the entire length of the ecotones.

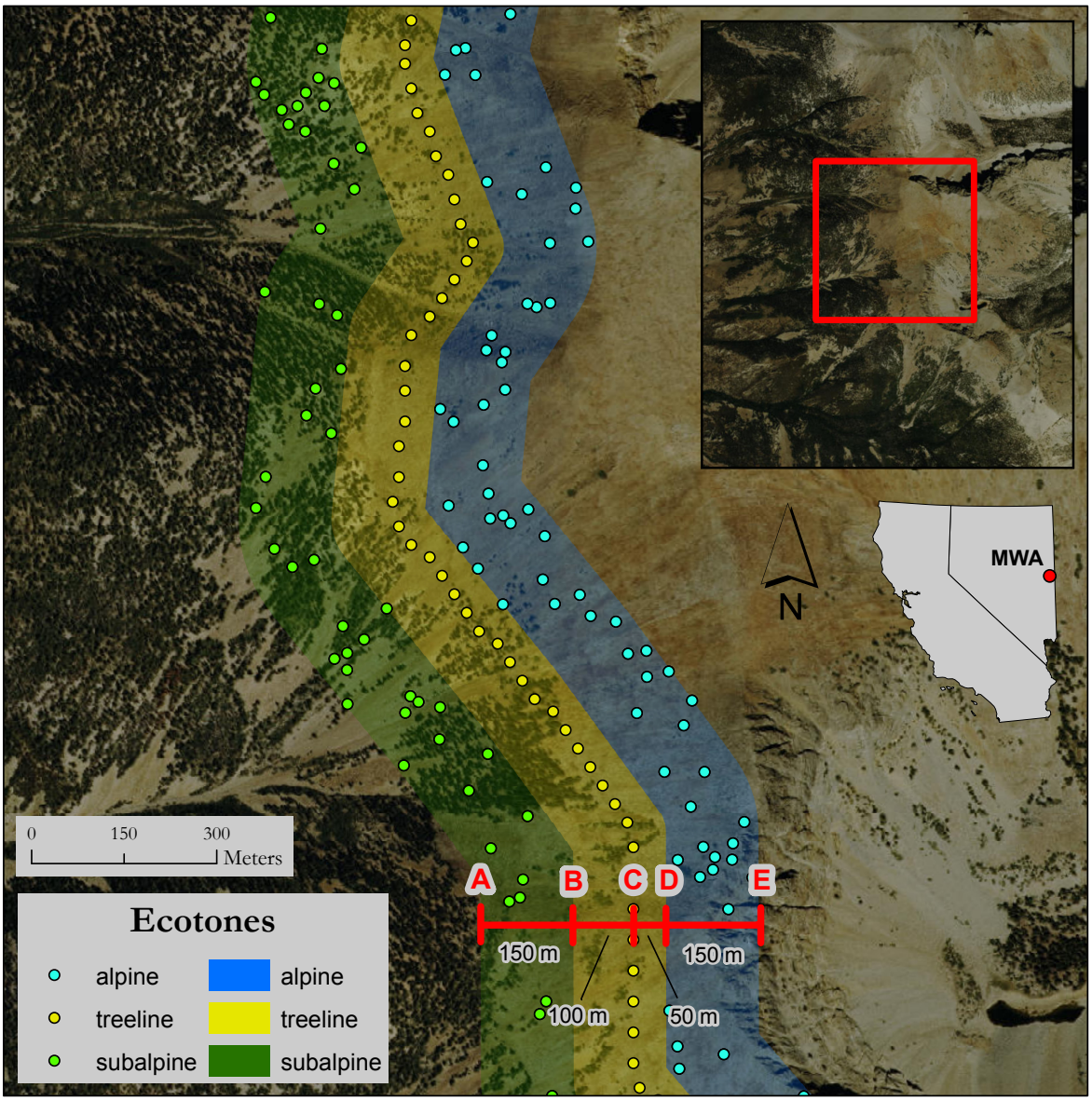

Figure 4: Digitized boundaries of the alpine, treeline, and subalpine ecotones, as described in section 2.5.1. These ecotones refer to the upper treeline as described in section 1.2 and are not related to the lower, moisture-limited treelines. **Note:** The subalpine ecotone's lower boundary (**A**) extends 150 meters upslope to the start of the treeline ecotone boundary (**B**). The treeline ecotone extends 150 meters upslope to the start of the alpine ecotone (**D**). The alpine ecotone extends 150 meters upslope with its upper boundary (**E**). Model training points for this ecotone are located at **C**, which lies 100 meters upslope from the lower treeline ecotone boundary (**B**), and 50 meters downslope from the upper treeline ecotone boundary (**D**). This is to ensure that all treeline ecotone model training points lie exactly within the treeline ecotone, due to the variable width of each ecotone due to changes in slope. See figure 5 for an example of how slope influences the width of each ecotone.

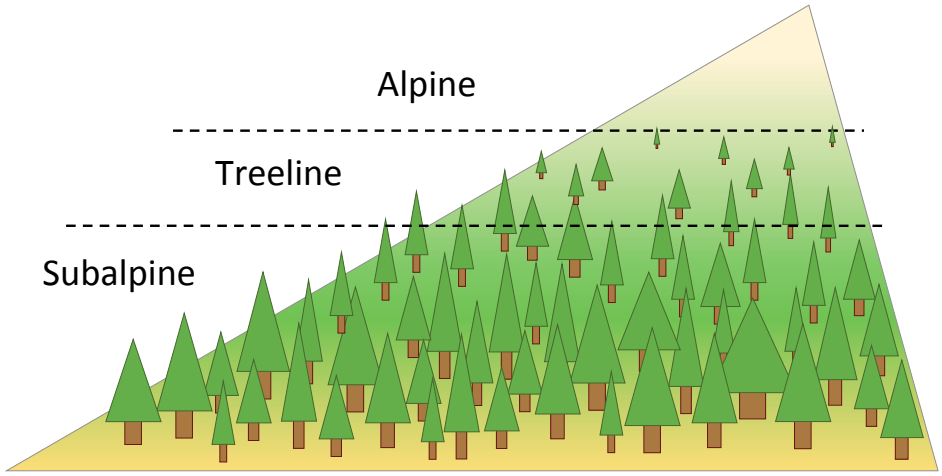

Figure 5: Conceptual diagram of the alpine, treeline, and subalpine ecotones, as described in section 2.5.1. These ecotones refer to the upper treeline as described in section 1.2 and are not related to the lower treelines formed by bristlecone and foxtail pine. Note the variable width (measured parallel to the mountain slope) of each ecotone depending on the slope.

2.5.2 Model Construction

With the training ecotones created, I generated a set of random points in the subalpine and alpine ecotones to extract climate data for the classification models. I extracted climate data for treeline ecotone from points along the actual tree*line* (explained in the above section and represented by letter C in figure 4) to ensure this data was the most representative of the treeline ecotone. I built a suite of preliminary classification models at each site. Each model had a different set of predictor variables, to identify the most influential variables for treeline prediction, and to implement Paulsen and Körner's (2014) methodology in a downscaled treeline model. The first model (MOD1) used all 60 topoclimate and 20 topography variables; the second model (MOD2) used only downscaled calculations of important treeline variables derived by Paulsen and Körner (2014); and a final set of models used the most effective predictive variables from MOD1 and MOD2. I used 20-fold cross validation in each individual model, and developed a strict pruning methodology to guard against over-fitting and maximize consistency between all the models. I pruned all models by setting a maximum branch

length of three splits, which inherently limits the number of possible splits in each branch to three, resulting in significantly fewer end nodes than an unpruned tree. Thus in the final classification algorithms, no final node could have more than three defining parameters. From a physiological perspective, the fewer splits and terminal nodes a classification tree has the simpler it is and easier to understand, allowing for meaningful comparisons between sites.

MOD1 used all 60 topoclimatic variables to identify the most important variables for prediction. MOD2 was then built using two temperature-derived treeline variables —the length of the growing season (LGS) and average temperature throughout it (SMT)—developed by Paulsen and Körner (2014). Their global treeline prediction model uses these variables to predict treeline position as a function of temperature. They define a minimum temperature needed (DTMIN) for cell division, with the assumption that cell division will occur only when the average daily temperature is above the threshold value. They subsequently define the growing season as all days with average temperature above DTMIN, sum the number of days within the growing season to find its length (LGS), and average the daily temperatures of all days within the growing season to find its seasonal mean temperature (SMT). Calculating these variables required daily resolved temperature data; Paulsen and Korner used cubic splines to interpolate daily values from monthly values obtained from a climate database. Following Paulsen and Körner's (2014) methodology, I used the monthly Tmean topoclimate maps to calculate the variables, yielding 10-meter resolution maps of both. I assumed the best fit for DTMIN (0.9 °C) calculated by Paulsen and Körner (2014) as our threshold value for calculations.

A set of 'final models' was then developed through an iterative process using combinations of the top three predictive variables from MOD1 and both treeline variables from MOD2, again with a maximum branch length of three nodes for each combination of variables. A single final model for each site was chosen by evaluating the resultant confusion matrices and Kappa statistics from the larger set of final models. In all cases, preference was given to models with a higher Kappa value and prediction accuracy, and fewer branches and predictive variables.

3 Results

3.1 Topoclimate Models

The topoclimate modeling yielded 60 unique temperature maps, consisting of five distinct variables modeled at monthly resolution. Generally, models are more accurate during the summer months (see R^2 values in tables 1 to 4). These treeline sites are harsh environments outside of the warmest summer months, with the possibility of snow pack existing well into late spring. Accordingly, several sensors at each site were covered by snow starting in late fall and in certain instances extending into May. Summer climate likely has the largest effect on treeline position and tree growth, so decreased accuracy throughout the winter months is not an issue. The following section describes general trends in the models for each climate variable; model accuracy and root mean square error for every individual model can be seen in tables 1 to 4. Sample predictions of June Tmin values are shown in figures 6 to 9, which show some of the trends described below (see figure captions for more details).

Elevation accounts for the largest amount of variance in the data, across all sites and for all variables. However, other variables in addition to elevation are significant predictors as well, varying by model and site. SHP is the exception to this trend, as elevation is by far the most effective predictor for all climate variables during the warmer months (May - October). MWA and PRL have the most similar topographic effects of any two sites, which is consistent with the similarities in regional geography between MWA and PRL. CSL is the site at which topography, rather than elevation, explains the most variance in the data.

Tmin models May - October are dominated by elevation at SHP, MWA, and PRL. At CSL, topographic convergence (TCI) and slope are the most effective predictors June - September (see figure 7). At MWA and PRL, TCI has influence over the late winter and spring models, yet elevation becomes the most effective predictor during the summer months. The SHP models are most influenced by elevation, yet TCI is still an influential factor throughout the year. Despite these differences, Tmin values model accurately at all sites, specifically during May - October, as nighttime cooling mechanisms are relatively predictable (Lookingbill and Urban 2003; Dobrowski et al. 2009). During these months, R^2 values range from 0.65 - 0.81 at

MWA, 0.66 - 0.81 at PRL, 0.82 - 0.87 at CSL, and 0.67 - 0.83 at SHP; and root mean square errors range from 0.24 - 0.27 °C at MWA, 0.33 - 0.44 °C at PRL, 0.20 - 0.27 °C at CSL, and 0.39 - 0.65 °C at SHP.

A similar effect is seen in the Tmean and DH5C models; elevation is the most dominant predictor all sites, while at CSL solar radiation loads are also significant for both Tmean and DH5C models. Typically, Tmean and DH5C models explain more variance with lower associated root mean square error at sites in which elevation is the most effective predictor. May - October Tmean R^2 values range from 0.64 - 0.81 at MWA, 0.66 - 0.91 at PRL, and 0.83 - 0.91 at SHP, and while CSL R^2 values range between 0.44 - 0.67. DH5C models behaved similarly, with May - October R^2 values ranging between between 0.39 - 0.72 at MWA, 0.64-0.86 at PRL, and 0.65 - 0.84 at SHP, while at CSL R^2 values range from 0.26 - 0.46.

Compared to the Tmin, Tmean and DH5C models, Tmax models indicate less explained variance, higher associated root mean square errors, and more inconsistency in topographic influence at all sites. The models at PRL and SHP perform slightly better than at MWA and CSL, perhaps a result of the greater influence of elevation in the PRL and SHP Tmax models. May - October Tmax R^2 values at MWA and CSL range from 0.36 - 0.54, and 0.27 - 0.46 respectfully, while at PRL and SHP R^2 values range from 0.41 - 0.73 at PRL and 0.77 - 0.83 at SHP. The DH5C models consistently explain more variance in the data than the Tmax models. Inconsistencies between the Tmin, Tmean, and Tmax models, and especially between the Tmax and DH5C models suggests different mechanisms for each variable, varying temporally (throughout the year) as well as spatially (site to site differences).

There is little consistency in the topographic effects within the DTR models, indicating the lack of a topographic mechanism controlling daily temperature swings at these sites. Consequently, topography and elevation account for only about half of the variance in the DTR models, which is less than most other variables.

Table 1: MWA topoclimate model R^2 and RMSE values, with boldface R^2 values over 0.60.

	Tmin		Tmean		Tmax		DTR		DH5C	
	R^2	RMSE	R^2	RMSE	R^2	RMSE	R^2	RMSE	R^2	RMSE
Jan	0.44	0.63	**0.69**	0.53	0.59	1.04	0.40	1.17	0.37	0.61
Feb	0.42	0.67	0.56	0.46	0.58	0.87	0.49	1.21	0.52	1.66
Mar	0.30	1.52	0.58	0.52	0.56	1.26	0.45	2.47	0.38	1.57
Apr	0.39	0.81	**0.63**	0.46	0.49	1.39	0.42	1.98	0.50	19.79
May	**0.65**	0.28	**0.64**	0.51	0.47	1.20	0.38	1.28	0.56	114.66
Jun	**0.78**	0.26	**0.69**	0.30	0.36	0.97	0.35	1.06	0.57	171.63
Jul	**0.80**	0.26	**0.74**	0.27	0.38	0.81	0.42	0.89	**0.72**	193.65
Aug	**0.79**	0.24	**0.74**	0.25	0.40	0.69	0.43	0.78	**0.68**	146.44
Sep	**0.78**	0.27	**0.76**	0.27	0.45	0.77	0.31	0.81	**0.70**	55.62
Oct	**0.81**	0.24	**0.81**	0.28	0.54	0.72	0.37	0.78	0.39	27.06
Nov	**0.68**	0.35	**0.69**	0.36	0.43	0.79	0.35	0.86	0.36	14.61
Dec	**0.62**	0.68	**0.63**	0.46	**0.67**	0.98	**0.63**	1.40	0.57	1.88

Table 2: PRL topoclimate model R^2 and RMSE values, with boldface R^2 values over 0.60.

	Tmin		Tmean		Tmax		DTR		DH5C	
	R^2	RMSE	R^2	RMSE	R^2	RMSE	R^2	RMSE	R^2	RMSE
Jan	0.42	0.67	**0.70**	0.54	**0.72**	0.88	0.56	1.04	**0.66**	0.86
Feb	0.41	1.18	0.55	0.79	**0.68**	0.84	0.56	1.27	**0.68**	0.42
Mar	0.33	1.74	0.42	1.00	**0.64**	1.15	0.53	2.15	**0.67**	0.26
Apr	0.40	1.39	**0.68**	0.69	**0.66**	1.18	0.47	2.16	**0.68**	11.05
May	**0.66**	0.44	**0.66**	0.85	0.56	1.80	0.48	1.87	**0.64**	147.69
Jun	**0.81**	0.41	**0.83**	0.61	**0.73**	1.19	0.38	1.49	**0.78**	203.09
Jul	**0.78**	0.44	**0.86**	0.38	0.41	0.93	0.37	0.98	**0.80**	273.71
Aug	**0.79**	0.33	**0.91**	0.24	**0.70**	0.57	0.57	0.71	**0.86**	186.33
Sep	**0.73**	0.35	**0.82**	0.25	0.57	0.59	0.43	0.68	**0.75**	94.41
Oct	**0.72**	0.34	**0.86**	0.30	**0.73**	0.63	0.59	0.65	**0.70**	27.63
Nov	**0.86**	0.32	**0.87**	0.35	**0.72**	0.70	0.45	0.67	**0.66**	12.89
Dec	0.33	0.77	**0.69**	0.51	**0.77**	0.67	0.54	0.94	**0.76**	1.10

Table 3: CSL topoclimate model R^2 and RMSE values, with boldface R^2 values over 0.60.

	Tmin		Tmean		Tmax		DTR		DH5C	
	R^2	RMSE	R^2	RMSE	R^2	RMSE	R^2	RMSE	R^2	RMSE
Jan	**0.75**	0.46	0.58	0.42	0.37	1.27	0.46	1.18	0.32	7.08
Feb	**0.73**	0.39	0.58	0.43	0.37	1.22	0.46	1.11	NA	NA
Mar	**0.75**	0.44	0.54	0.37	0.42	1.06	0.56	0.96	0.32	16.43
Apr	**0.75**	0.24	0.49	0.30	0.41	0.88	0.53	0.81	0.38	54.33
May	**0.82**	0.20	**0.67**	0.27	0.41	0.80	0.55	0.75	0.39	80.95
Jun	**0.83**	0.27	**0.63**	0.26	0.46	0.74	**0.65**	0.71	0.46	167.58
Jul	**0.83**	0.23	**0.65**	0.24	0.41	0.76	0.59	0.72	0.40	168.11
Aug	**0.87**	0.25	**0.60**	0.32	0.38	0.98	0.57	0.93	0.38	252.81
Sep	**0.86**	0.24	0.54	0.35	0.35	0.94	0.54	0.90	0.34	81.07
Oct	**0.83**	0.27	0.44	0.33	0.27	1.13	0.46	1.09	0.26	137.20
Nov	**0.79**	0.27	0.53	0.31	0.23	1.23	0.30	1.16	0.25	83.58
Dec	**0.72**	0.47	**0.62**	0.32	0.33	1.00	0.51	1.05	0.27	25.87

Table 4: SHP topoclimate model R^2 and RMSE values, with boldface R^2 values over 0.60.

	Tmin		Tmean		Tmax		DTR		DH5C	
	R^2	RMSE	R^2	RMSE	R^2	RMSE	R^2	RMSE	R^2	RMSE
Jan	**0.66**	0.66	**0.81**	0.40	**0.73**	0.76	**0.71**	0.85	**0.69**	4.33
Feb	**0.73**	0.52	**0.89**	0.32	**0.71**	0.86	**0.67**	0.89	0.56	4.58
Mar	**0.70**	0.64	**0.84**	0.40	**0.68**	1.00	**0.64**	1.18	**0.61**	56.50
Apr	**0.78**	0.38	**0.88**	0.34	**0.81**	0.89	**0.80**	0.82	**0.81**	64.82
May	**0.83**	0.39	**0.91**	0.32	**0.83**	0.68	**0.76**	0.65	**0.77**	100.45
Jun	**0.67**	0.65	**0.85**	0.36	**0.78**	0.99	**0.77**	1.11	**0.84**	214.26
Jul	**0.78**	0.40	**0.87**	0.32	**0.79**	0.87	**0.72**	0.99	**0.80**	240.08
Aug	**0.72**	0.57	**0.85**	0.36	**0.77**	0.98	**0.84**	0.88	**0.76**	306.84
Sep	**0.73**	0.61	**0.83**	0.40	**0.83**	0.76	**0.84**	0.84	**0.83**	60.64
Oct	**0.80**	0.52	**0.84**	0.37	**0.78**	0.76	**0.77**	0.90	**0.65**	104.11
Nov	**0.78**	0.43	**0.85**	0.33	**0.65**	0.88	**0.64**	0.91	**0.66**	63.41
Dec	**0.78**	0.42	**0.87**	0.32	**0.81**	0.57	**0.78**	0.56	**0.80**	5.97

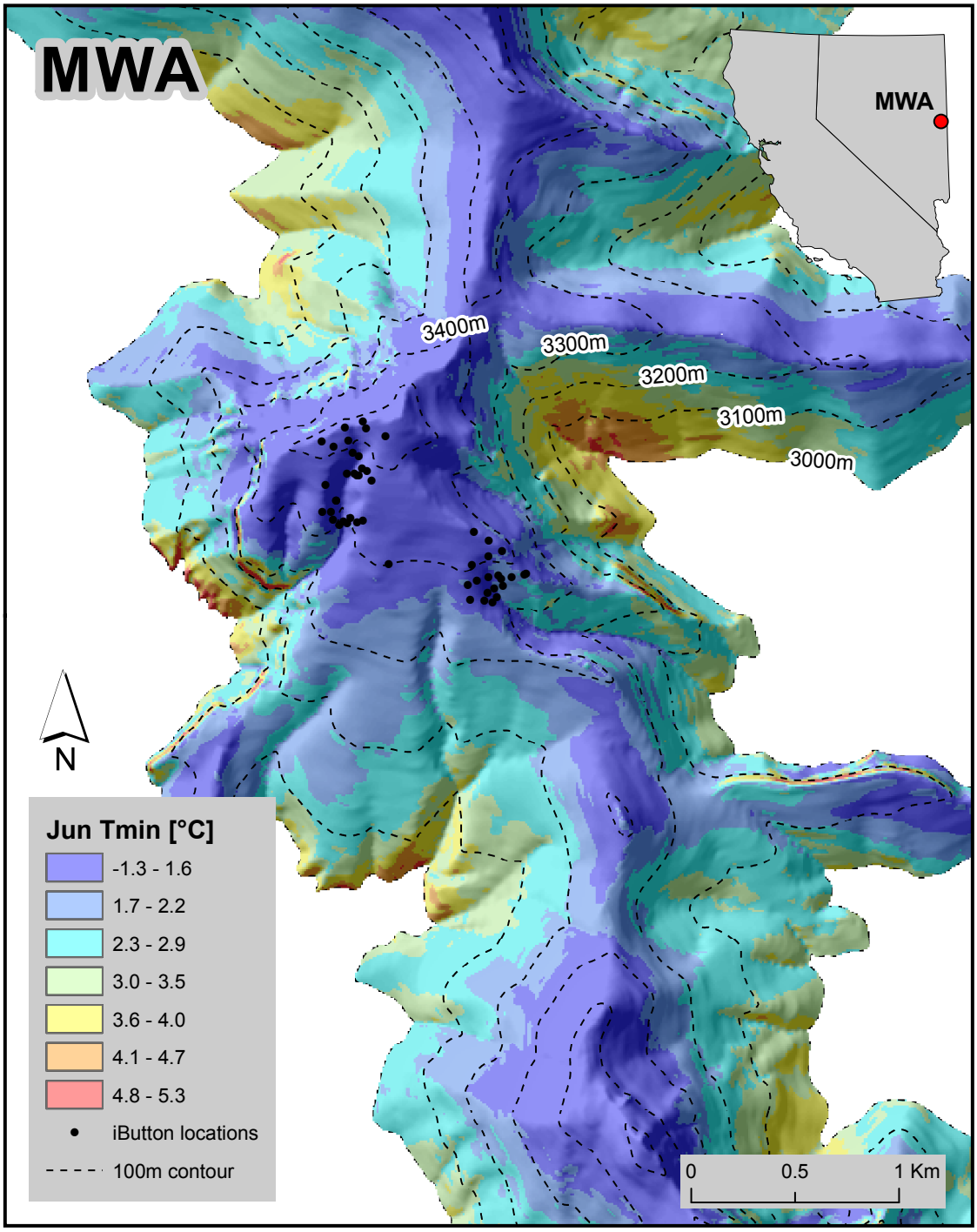

Figure 6: June Tmin models at MWA with iButton locations and dotted contour lines.

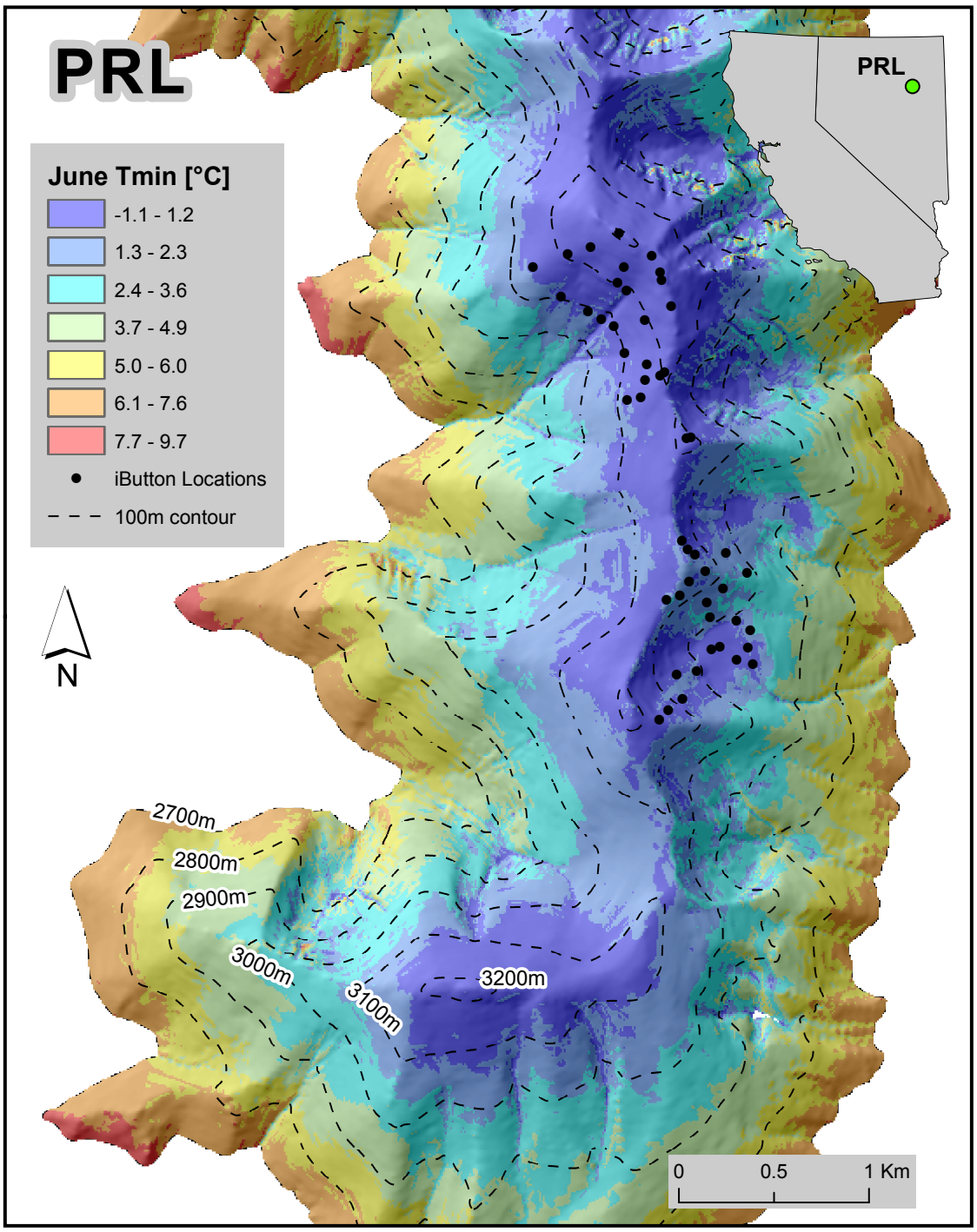

Figure 7: June Tmin models at PRL with iButton locations and dotted contour lines.

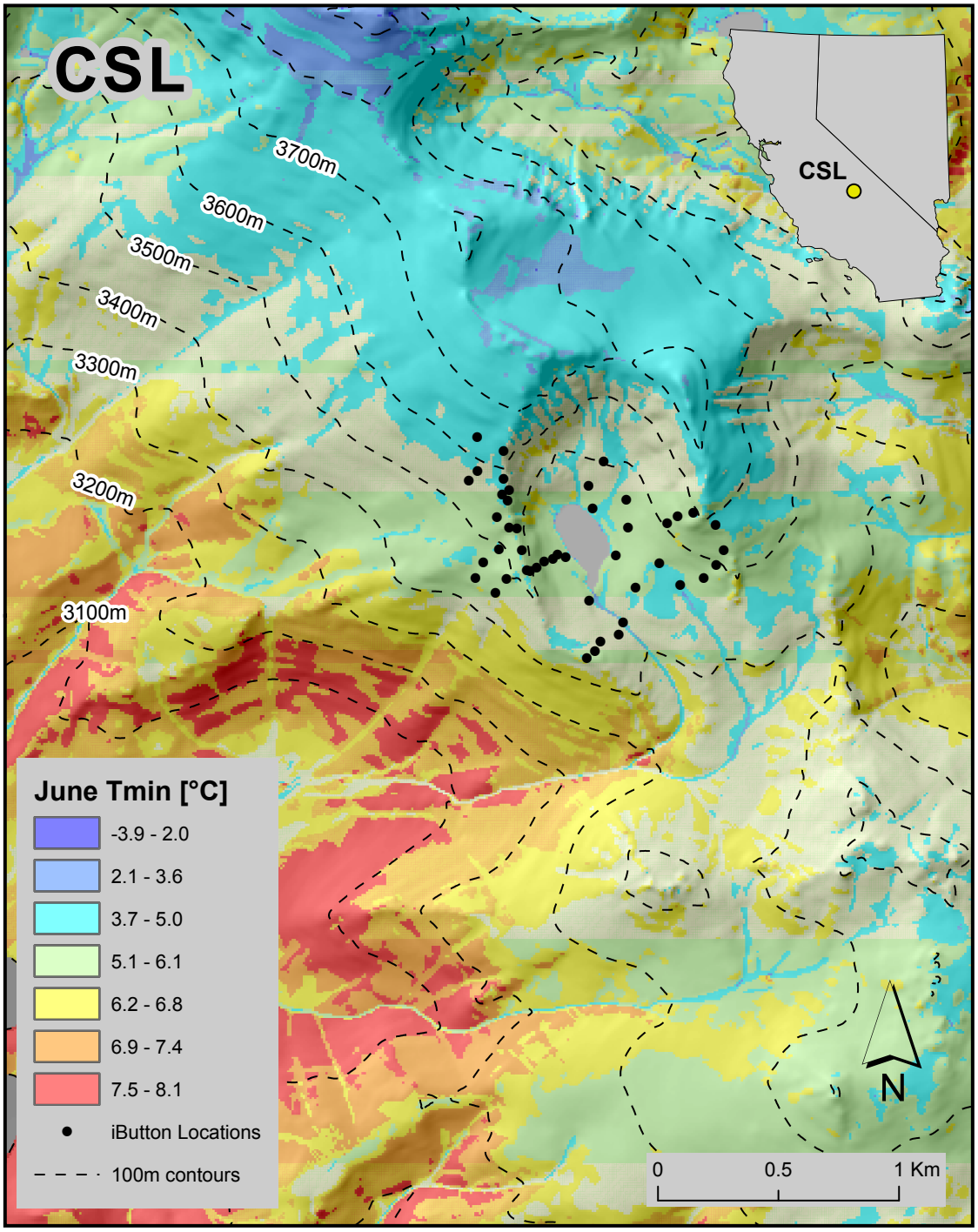

Figure 8: June Tmin models at CSL with iButton locations and dotted contour lines.

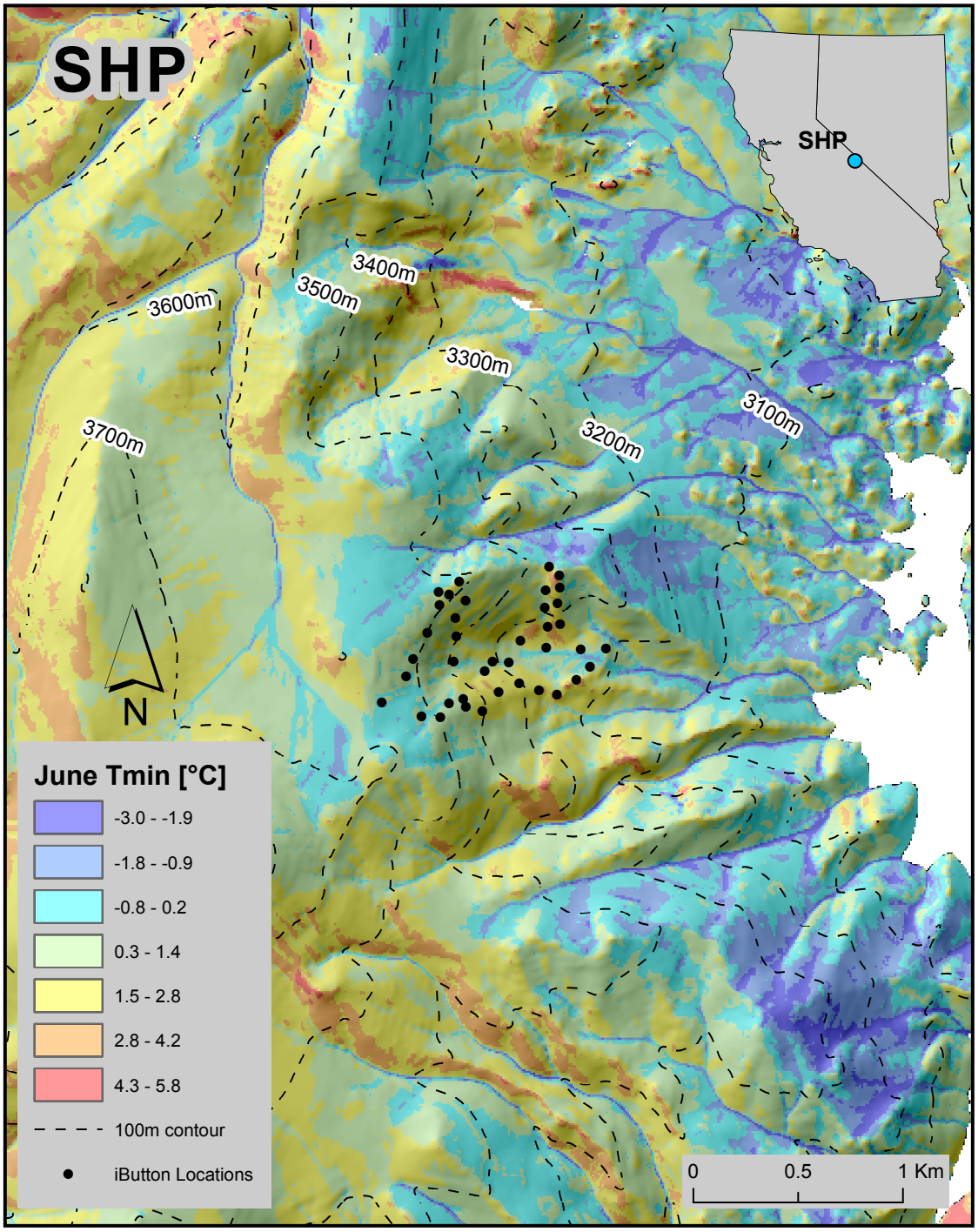

Figure 9: June Tmin models at SHP with iButton locations and dotted contour lines.

3.2 Classification Models

Finalized classification trees for each site can be seen in figures 10 to 12. Results between the sites vary slightly, indicating different specific variables as effective treeline position predictors at each site. However as a whole, these findings add evidence that treeline position is influenced by temperatures during the growing season, and that *in situ* measurements can lend insights to differences in individual treeline position, as well as quantifying physiological limits of bristlecone and foxtail pines.

3.2.1 Classification Algorithms

At SHP and CSL, May and April Tmean proved the most effective predictor of treeline position respectively (figures 11 and 12), while at MWA July DH5C was most important (figure 10). MWA was the only site at which either LGS or SMT played a role in the models.

At MWA, values of July DH5C are used to make the primary split in the data, inferring that July DH5C is the most important predictive variable at MWA (figure 10). The effects of LGS and SMT are also present, as these variables are used in secondary and tertiary splits. While the treeline ecotone is modeled by three distinct algorithms, they are not weighted equally, with one algorithm containing a vast majority (163/220) of the training points from the treeline ecotone. This primary climate envelope for the treeline ecotone requires July DH5C values to be less than 4233 degree hours, with a growing season average temperature (SMT) below 7.35 °C and a growing season length exceeding 144 days (LGS). This algorithm separates the treeline ecotone from the alpine ecotone, and is seen on the left side of figure 10. The remaining, secondary climate envelopes for the treeline ecotone separate it from the subalpine ecotone. The first requires July DH5C values above 4421 degree hours, and August DH5C values below 3741 degree hours, while the second requires July DH5C values between 4233 and 4421 degree hours, and a growing season longer than 155 days. Treeline producer accuracy in this model is 85%, while consumer accuracy is lower, around 54% (table 5). The treeline ecotone is over predicted into the alpine ecotone, as consumer accuracy for the alpine ecotone very high at 98%, compared to the producer accuracy of 47% (table 5). The subalpine

ecotone is predicted reasonably well, with a consumer accuracy of 88% and a producer accuracy of 82% (table 5). A kappa statistic of 0.61 indicates substantial agreement that these results are different than a random expectation, and overall model accuracy is 74% (table 5).

The CSL classification model is markedly different than the MWA model, with the treeline ecotone contained by a single climate envelope, and without the influence of LGS or SMT (figure 11). At CSL, values of Tmean are important predictors, specifically April Tmean. This variable is used to make the primary split in the training points, and separates most (228/385) of the alpine training points from the treeline and subalpine points. The treeline algorithm requires values of April Tmean greater than -4.09 °C, July Tmean values less than 7.88 °C, and values of September Tmean greater 4.18 °C. Treeline producer accuracy is 46%, while the consumer accuracy is higher at 63% (table 6). This model over predicts the subalpine ecotone into the treeline ecotone, which is apparent in classification ratio shown at the terminal node of the subaline ecotone within figure 11. A kappa statistic of 0.46 indicates moderate agreement that these results are different than a random expectation, and overall model accuracy is 64% (table 6).

The classification model at SHP is similar to that at CSL, containing a single treeline climate envelope and excluding the influence of LGS or SMT in the classification algorithms (figure 12). Interestingly, only one variable was used to build the most accurate model, May Tmean, with only 2 splits. The treeline ecotone is predicted with an algorithm that requires May Tmean temperautres between 0.16 °C and 1.01. Despite the simplicity of this model, it is the least accurate of all three classification models, over predicting the alpine ecotone and significantly under predicting the subalpine ecotone. Treeline classification accuracies hover around 50%, with a consumer accuracy of 53% and a producer accuracy of 52% (table 7). A kappa statistic of 0.30 indicates fair agreement that these results are different than a random expectation, and overall model accuracy is 53% (table 7).

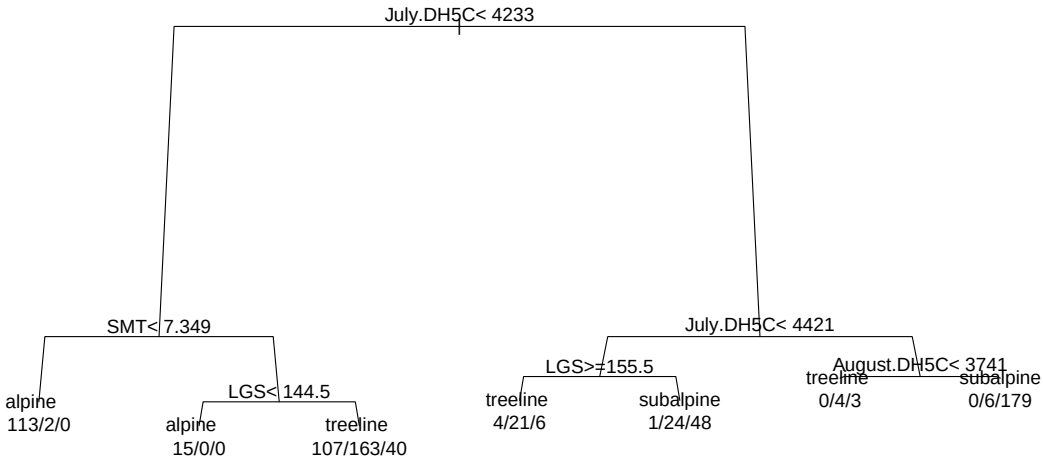

Figure 10: Final classification model at Mount Washington, NV, located in the Snake Mountain Range. The text above each split indicates the threshold values used to separate the ecotones for that split in the model. In this model the primary split uses a threshold of July DH5C < 4233 degree hours, meaning all terminal nodes on the left side of this split have July DH5C values fewer than 4233 degree hours, and terminal nodes on the right of this split have July DH5C values greater than 4233 degree hours. The secondary and tertiary splits use other variables to further distinguish the ecotone boundaries: the growing season length (LGS), growing season average temperature (SMT), and August degree hours above 5 °C. This model is the most accurate of the three sites in this analysis, with substantial agreement this result is different than a random classification. Numbers below each terminal node in the tree represent the number of points from each ecotone (in the order of 'alpine/treeline/subalpine') that are included in this model's classification. For example, the left-most terminal node is classified as alpine, and the numbers below represent the ratio of points from each ecotone that are classified as part of the alpine ecotone by this branch in the model: there are 113 alpine points (correctly classified in this case), 2 treeline points (incorrectly classified), and 0 subalpine points.

Table 5: Confusion matrix for the classification model shown in figure 10. Cohen's kappa value of 0.61 indicates substantial agreement the classification is different than random. Notice only one misclassification of an alpine point as subalpine, and no misclassification of subalpine as alpine. The largest area of misclassification predicts alpine regions as treeline, indicating the model over predicts the treeline ecotone into the alpine region.

		Actual			
		alpine	**treeline**	**subalpine**	Consumer error
Predicted	**alpine**	**128**	2	0	0.02
	treeline	111	**188**	49	0.46
	subalpine	1	30	**227**	0.12
	Producer Error	0.47	0.15	0.18	Kappa = 0.61

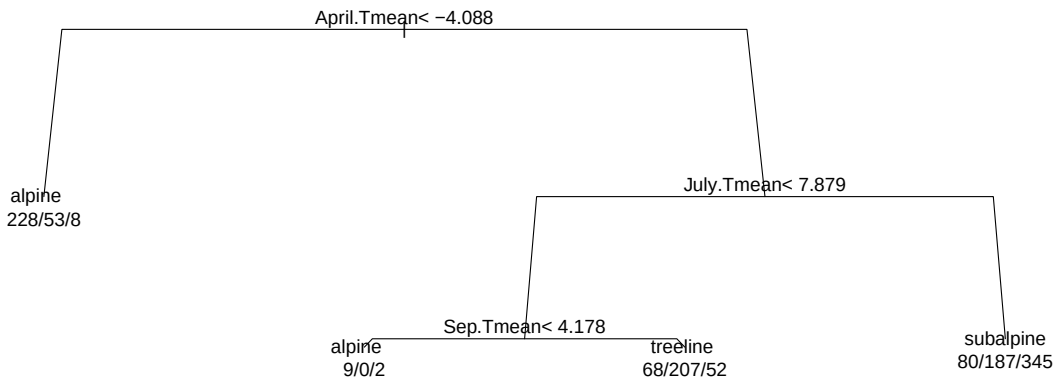

Figure 11: Final classification model at Chicken Spring Lake, in the Sierra Nevada mountains in California. The text above each split indicates the threshold values used to separate the ecotones for that split in the model. In this model, the primary split uses a threshold of April Tmean below -4.09 °C, meaning all terminal nodes on the left side of this split have average April temperatures less than -4.09 °C, and all terminal nodes on the right of this split have average April temperatures greater than -4.09 °C. This first split classifies all regions with average April temperatures below -4.09 °C as alpine. The secondary split in the model classifies all regions with July average temperatures above 7.88 °C as subalpine. Numbers below each terminal node in the tree represent the number of points from each ecotone (in the order of 'alpine/treeline/subalpine') that are included in this model's classification. For example, the left-most terminal node is classified as alpine, and the numbers below represent the ratio of points from each ecotone that are classified as part of the alpine ecotone by this branch in the model: there are 228 alpine points (correctly classified in this case), 53 treeline points (incorrectly classified), and 8 subalpine points (incorrectly classified).

Table 6: Confusion matrix for the classification model shown in figure 11. Cohen's kappa value of 0.46 indicates moderate agreement the classification is different than random. While there is moderate misclassification between neighboring ecotones, the most frequent error comes from misclassifying treeline regions as subalpine, inferring the treeline ecotone is under predicted in by this model.

		Actual			
		alpine	**treeline**	**subalpine**	Consumer error
Predicted	**alpine**	**237**	53	10	0.21
	treeline	68	**207**	52	0.37
	subalpine	80	187	**345**	0.44
	Producer Error	0.38	0.54	0.15	Kappa = 0.46

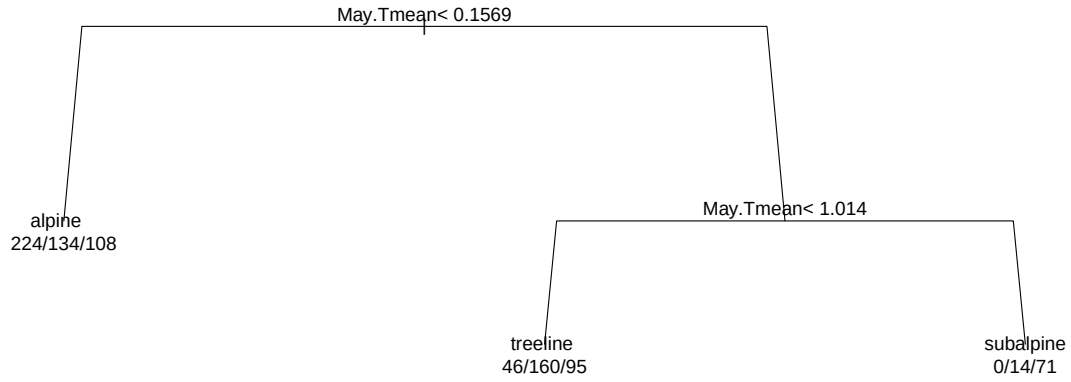

Figure 12: Final classification model at Sheep Mountain, in the White Mountains of California. The text above each split indicates the threshold values used to separate the ecotones for that split in the model. In this model, the primary split uses a threshold of May Tmean below 0.15 °C, meaning all terminal nodes on the left side of this split have average May temperatures less than 0.15 °C, and all terminal nodes on the right of this split have average May temperatures greater than 0.15 °C. This first split classifies all regions with average May temperatures below 0.15 °C as alpine. The secondary split in the model classifies all regions with May average temperatures above 1.01 °C as subalpine, and thus predicting the treeline ecotone as all regions with average May temperatures between 0.15 °C and 1.01 °C. Numbers below each terminal node in the tree represent the number of points from each ecotone (in the order of 'alpine/treeline/subalpine') that are included in this model's classification. For example, the left-most terminal node is classified as alpine, and the numbers below represent the ratio of points from each ecotone that are classified as part of the alpine ecotone by this branch in the model: there are 224 alpine points (correctly classified in this case), 134 treeline points (incorrectly classified), and 108 subalpine points (incorrectly classified).

Table 7: Confusion matrix for the classification model shown in figure 12. Cohen's kappa value of 0.30 indicates fair agreement the classification is different than random. There is substantial misclassification between most ecotones, indicating the decreased power of this model as compared to the models at CSL and MWA.

		Actual			
		alpine	**treeline**	**subalpine**	Consumer error
Predicted	**alpine**	**224**	134	108	0.52
	treeline	46	**160**	95	0.47
	subalpine	0	14	**71**	0.16
	Producer Error	0.17	0.48	0.74	Kappa = 0.30

4 Discussion

The objectives of my analysis are threefold:

1. Identify physical controls on surface temperatures in rugged mountainous terrain, specifically striving to identify the influence of *diverse topography*—separate from changes in elevation—on daily patterns of warming and cooling

2. Use modeled climate variables to predict the position of climate-limited treelines in the Great Basin

3. Identify physiological thresholds that limit bristlecone and foxtail pine growth at the highest elevations and cause climate-limited treelines to form in the Great Basin, and compare these thresholds to other treeline locations globally.

The following sections address the extent to which my results provide reliable answers to these questions, how this information may contribute to the research community, and how the implications of this work may influence future studies.

4.1 Elevation as a proxy for temperature

The use of elevation as a proxy for temperature in complex terrain is potentially fraught with error. At global and regional scales, elevation can be used reliably as a proxy for temperature if accurate measures of regional lapse rates can be obtained; Paulsen and Körner (2014) successfully use elevation to adjust coarse-resolution temperatures at 376 cites in their treeline position model. However, at smaller scales (meters to kilometers) topography influences temperatures greatly, and elevation-induced trends in warming and cooling are not consistent spatially or temporally (Lookingbill and Urban 2003; Dobrowski et al. 2009; Weiss et al. 2015). My results corroborate these findings; while elevation is the best predictor of most climate variables, other topographic variables were also important in many models. Elevation can be a useful proxy of temperature at the appropriate scale, yet at the landscape scale topography is necessary to explain spatial differences in temperature while elevation remains constant. See figures 8 and 9 for examples of how temperatures change while elevation remains constant.

4.2 Topographic influences on temperature

It is important to clarify the distinction between the influences of elevation and topography in the topoclimate models; the effect elevation has on temperatures at these sites in not considered a topographic effect, as the objective of this analysis is to identify topographic controls on temperatures *independent* of elevation. While elevation is related to many of the topographic predictor variables used here, its primary effects are discussed above

The models typically explain more variance in Tmin than Tmax. Daily minimum temperatures consistently occur during the pre-dawn hours, as radiative cooling occurs throughout the night, typically resulting in the lowest daily temperatures just before sunrise. Conversely, daily maximum temperatures usually occur in the late afternoon—lagging several hours behind peak solar radiation loads—as heat capacity of the landscape continues to warm the air even after peak solar radiation loading. Accordingly, the Tmin training values represent a month's average daily low temperature occurring during the pre-dawn hours, while the Tmax training values represent a month's average daily high temperature, occurring in late afternoon. The inconsistencies in model performance between these two metrics stem from the different mechanisms that control night-time minimum temperatures and day-time maximum temperatures.

The most important topographic predictor of Tmin is topographic convergence (TCI). On shaded slopes temperatures fall throughout the late afternoon and evening as incoming solar radiation decreases and the radiative balance shifts from positive to negative. Consequently, air directly above the ground begins to cool as long wave radiation is emitted from the Earth's surface throughout the night (Geiger et al. 2009). These slight temperature differences drive surface-air density gradients near the ground, and the cooler denser air begins to flow downhill, following natural drainage pathways on the landscape. If stable weather conditions exist, this easily predictable pattern of Katabatic flow can dominate the night-time climate (Geiger et al. 2009). Originally developed as a corollary for soil moisture, TCI is a reliable proxy for cold air drainage, as it relates up slope watershed area to the slope at a specific location (Wolock and McCabe 1995). Areas that are flatter with large areas of upslope-contributing area will

have more pooling of cool dense air flow than steeper areas without converging topography to channel the flowing air; this assumes that cool air flows and pools similarly to a viscous liquid (Geiger et al. 2009), and has been demonstrated to have observable effects on physical systems (Dobrowski et al. 2009) and biological systems (Adams et al. 2014; Bunn et al. 2011). These effects are best demonstrated at CSL; topographic convergence is most important predictor of Tmin June - October (more so than elevation), and is in the top three predictors for all months except May. While TCI remains an important predictor of Tmin during the spring months at all sites, elevation becomes the most important predictor during the warmer summer months, suggesting that at MWA, PRL, and SHP, summer nighttime low temperatures may decouple from the surrounding topography and follow local lapse rates more closely.

In contrast to Tmin's consistent predictability, Tmax prediction was less accurate and inconsistent. Daily maximum temperatures are heavily influenced by solar radiation loading, which is sensitive to different physical and environmental factors (Lookingbill and Urban 2003; Chung and Yun 2004; Geiger et al. 2009). The sensors were covered by radiation shields and mounted on the north side of the tree to decrease the effect of direct sunlight on the measured air temperatures, yet there is likely some residual effect of direct sunlight striking the radiation shields, as the amount of time each sensor and its radiation shield were in direct sunlight differs between sensors. Additionally, there may have been slight differences in shading between sensors not directly represented in the topographic predictor data. As radiation loads increase throughout the day and warm the landscape, air near ground becomes warmer and starts to rise. This results in mixing and reliably unpredictable airflow acting to reduce temperature gradients (S. B. Weiss, 2016, personal communication). All of these factors add significant noise to the Tmax data, resulting in less explained variance than the Tmin data.

It appears that a daily average calculation of the hourly temperatures may act to smooth out varying topographic effects on daily minimum and maximum temperatures, and closely follows warming and cooling trends driven by changes in elevation. For example, June Tmin and Tmax values are the average of thirty daily minimums and maximums, while the Tmean metric is representative of the average hourly June temperature. The Tmean metric is in-

herently more representative of the entire month's climate, rather than targeted to represent specific warming or cooling mechanisms. Thus, it follows that Tmean is best predicted by changes in elevation as the specific topographic influences of day-time warming and night-time cooling are diminished, as neither mechanism influences all the hourly data, while the influences of elevation are always present.

A similar effect can be seen in the DH5C models. This integrated measure of temperatures is typically best explained by changes in elevation, although the aspect-derived eastness index and solar radiation loads also add to the models. Daily warming trends are greatly effected by solar radiation loads, explaining the importance of these terms in the DH5C models. Eastness may be influential because east-facing slopes receive direct sunlight before other aspects, causing the radiative balance on these slopes to shift from negative to positive earlier in the day, allowing for longer periods of time with temperatures above 5 °C (S. B. Weiss, 2015, personal communication).

There was little consistency in the topographic effects on DTR values, indicating the lack of a cross-site mechanism driving diurnal temperature ranges. Interestingly, from May - October when models at CSL explain roughly 50% of the variance in the DTR values, TPI_{25}, TPI_{50} were consistently the most effective predictors. The TPI indices represent how different the elevation is at a given location relative to the surrounding area on small scales, within circles with radii of 25 and 50 meters. These results may indicate rugged areas with larger changes in elevation across small horizontal distances (such as steep canyons or deep glacial cirques, etc) provide increased shading which acts to dampen the effects of radiation and day-time warming, resulting in lower temperature swings throughout the day. Less rugged areas will have lower temperatures during the night as radiative cooling is greatest in locations with more exposure to open sky, and higher solar radiation loads during the day without shading from topographic features, perhaps leading to greater differences between the daily minimum and maximum temperatures.

4.3 Global vs. Regional Treeline models

The value of the global TREELIM model is that it calculated a set of simple parameters that constrain treeline positions formed by many different treeline-forming species across many diverse climatic zones. Agreement between results from TREELIM and an independent data logging campaign by Körner and Paulsen (2004) provide strong evidence for a common biological limit constraining tree growth across all treeline-forming species. Paulsen and Körner (2014) guard against interpreting these results too literally—the model calculates a best fit of 6.4 °C as "a common isotherm of low temperature for forest limits", yet they stress the lack of physiological relevance represented by this value. While it is close to the physiological limit for woody biomass accumulation, they argue it "reflects an arithmetic mean that is subsuming the combined action of low temperature, integrated over time, on a suite of processes associated with tissue formation, from root tips to apical meristems". With this understood, the regional treeline positions and characteristics at MWA, CSL, and SHP can be viewed from the global, mechanistic perspective.

The LGS and SMT topoclimate maps at my sites suggest the isotherm influencing treeline position reported by Paulsen and Körner (2014) is consistent in the Great Basin, while the length of the growing season may be longer. Table 8 shows values of LGS and SMT extracted from the treeline position used to build the treeline ecotone at each site (see section 2.5.1). Values of SMT are very similar to the 6.4 °C calculated from TREELIM, however it is important to note that these values represent SMT during period of treeline position stabilization, and are cooler than values of SMT if calculated from the current climate. Conversely, my models show Great Basin treeline growing season is likely longer than at other treeline locations—perhaps a result of the arid climate. Korñer and colleagues repeatedly stress the presence of a common isotherm at treeline sites globally, and focuses less attention on the length of the growing season as a driving factor of treeline position; multiple studies provide evidence supporting the presence of a common isotherm at treelines, while growing season lengths differ significantly (Körner and Paulsen 2004; Körner 2007, 2012; Paulsen and Körner 2014). This body of research seems to suggest treeline position is influenced more by the

average temperature during the growing season than its length. My results would corroborate this; the Great Basin treeline sites values of LGS are greater than TREELIM's best fit by 52% - 62%, while values of SMT are within 1.2 °C of TREELIM's best fit. Further, TREELIM's reported values are a global average of LGS and SMT calculated from many different species, and values specific to any one species are likely different from this average.

	TREELIM	MWA	CSL	SHP
LGS [days]	**94**	152	146	143
SMT [°C]	**6.4**	7.6	5.5	6.3

Table 8: Values of treeline predicting variables developed by Paulsen and Körner (2014). Shows comparisons between the global average of 376 treeline sites used in the TREELIM model, and values from MWA, CSL, and SHP.

4.4 Topoclimate Prediction of Treeline Position

Despite the importance of TREELIM as a global treeline position model, the authors address its main shortcoming as the lack of physiological meaning captured by its predictive variables. Other studies have reached similar conclusions regarding direct temperature values (measured in °C or F) as a treeline predictive variable Jobbagy and Jackson (2000); Weiss et al. (2015). The value of site-specific treeline analysis is in the ability to employ variables that may more accurately explain a physiological mechanism for treeline formation—however this work would not be possible without the information and insight gained from the global analyses that precede it. My analysis is unique in that it includes degree hour calculations, in addition to direct temperature values, as treeline-predictive variables. Degree hour calculations have been shown to have a more direct influence on plant physiology (Sykes et al. 1996; Körner 2008), and thus may also be useful for treeline prediction. Körner (2008) specifically cites values of degree hours above 5 °C as a potential constraining factor of alpine treelines, evidenced through an analysis of winter physiological activity in crops.

A different topoclimate variable was the best treeline position predictor at the sites presented in this analysis. These results are not cause for alarm, as individual treelines may likely be influenced by slightly different factors, and interactions between each treeline and site-specific characteristics are possible. Yet, these results are in strong agreement with the

general theory for climatic treeline formation, and may provide new evidence for a mechanism rooted in tree physiology. The treeline position at MWA was most accurately predicted by July DH5C, while CSL and SHP treelines were most accurately predicted by April and May Tmean, respectively. In this analysis, Tmean and DH5C are more descriptive than Tmin or Tmax, in that more of the hourly data was used in their calculation, and thus may be more representative of the overall climate for a given location. The influence of the LGS and SMT on the models is inconsistent between sites—MWA was the only site at which the models included these variables, indicating the down-scaling methods used in this analysis to calculate LGS and SMT may weaken their predictive ability. Additionally, individual treeline positions may be subject to complex interactions, as regional weather patterns, topographic features, or other factors may be less influential on a global scale. Results from the topoclimate modeling of climate variables support this; the importance of elevation and specific topographic features varied by site for each modeled variable, showing spatial variation in the topographic controls on each variable. These differences may depend on the regional meteorology and climate at each site, as well as differences in larger-scale geography and local topographic features. As the factors influencing topoclimate vary spatially, it follows that the factors controlling treeline position at the same scale vary spatially as well.

Physiologically, values of degree hours above 5 °C are more meaningful as a predictive variable than a direct temperature measurement. Given the right conditions, two treeline sites may have the same average temperature for a given month while values of degree hour calculations may be quite different. Much of the current treeline literature references the importance of growing season length on treeline position—in effect the DH5C variable provides similar information about the duration of the growing season. The main difference is that the DH5C variable represents the total number of degrees per hour that temperatures are above 5 °C, while the length of the growing season only represents the number of days temperatures are above a given threshold. This presents a similar problem with LGS as a predictive variable; in the right conditions two treeline sites with similar growing season lengths could have drastically different values of DH5C. A more appropriate definition of growing season length with respect to climatic treelines may incorporate a measure of degree hours, rather than days

with average temperature above a specified threshold. This highlights the benefits of a local treeline analysis, as hourly data enable a DH5C calculation that—at MWA—more accurately predicts the treeline position than an direct measure of temperature.

4.5 Classification model structure and performance

Classification trees seen in figures 10 to 12 show the similarity in structure between the CSL and SHP models, and their stark contrast to the model at MWA. CSL and SHP are more similar to each other than to MWA or PRL, sharing several main characteristics. The striking difference between the California sites and the Nevada sites is their respective regional geographies. The Sierra Nevada (CSL) and White Mountain (SHP) ranges are significantly larger than the Snake (MWA) and Ruby (PRL) ranges, and have a different effect on moving air masses and the regional meteorology. There is significantly more land mass above 3000 meters at CSL and SHP, with vast stretches of alpine area above treeline. Conversely, MWA and PRL are characteristic of the sky island ranges in the central Great Basin, with treeline position at or just below the highest reaches of each mountain range. These sites quickly drop off thousands of meters to the desert valley floor below, and have much less overall area above 3000 meters than CSL and SHP. Additionally, SHP and CSL have cooler, more moderate climates, while MWA and PRL have warmer more extreme climates.

These differences in geography and climate between the sites may account for the similarity in results between CSL and SHP and the differences between these sites and the results at MWA, for both model accuracy and the important treeline predicting variables. MWA is the most different of the treeline models, with the highest overall accuracy, the most complex classification tree, and interestingly the only site at which LGS and SMT played a roll in the classification algorithms. July DH5C, and to some extent August DH5C, separate the subalpine training points from the treeline and alpine points quite well, indicating more climatological similarity between the treeline and alpine ecotones than between the treeline and subalipine ecotone. Additionally, most of the misclassification in the MWA model resulted from separating the alpine from the treeline points. Interestingly, these separations are completed by the LGS and SMT variables, rather than the modeled topoclimate variables. Results

indicate that the alpine and treeline ecotones are more similar, and markedly different than the subalpine ecotone.

Results from CSL and SHP are different—both models' primary split separates the alpine ectotone from the treeline and subalpine ecotones, indicating greater climatological similarity between the treeline and subalpine ecotone at these sites. This primary separation between the alpine ecotone and the treeline and subalpine ecotones is in contrast to the MWA model. Furthermore, CSL and SHP models use April and May Tmean values respectively to create the primary split, another contrast to the MWA model which uses July DH5C. The CSL and SHP models do not find as stark a contrast between alpine ecotone and the treeline and subalpine ecotones as the MWA model does between the alpine and treeline ecotones, and the subalpine ecotone. The CSL model's primary split classifies 228 out of 289 correctly as the alpine ecotone, while the SHP model classifies only 224 out of 466 correctly as alpine. The secondary and tertiary splits in these models then separate the treeline points from the subalpine points.

Each model easily separates the most dissimilar ecotone from the other two in the primary split, with most of the misclassification resulting from separating the two ecotones that are more similar via the secondary and tertiary splits. Despite the differences between sites, taken as a whole these results indicate measurable dissimilarity between the alpine and subalpine ecotones, with the treeline ecotone falling somewhere in between. The fact that the treeline ecotone is more similar to the alpine ecotone at MWA, and the subalpine ecotone at CSL and SHP is less important than the main finding that there seem to be two, rather than three ecotones at these locations. The treeline ecotone is a transition zone, the boundary between the the alpine and subalpine ecotones, and is accordingly difficult to model as its own distinct entity. Thus, future analyses repeating the methods presented in this analysis may find more success in treeline position modeling using only two ecotones, with the treeline position as the boundary between the alpine and subalpine ecotone.

4.6 Implications

The climate data used to build the classification models was adjusted to represent average annual conditions during the period of current treeline position stabilization in the Great Basin—around 1328 A.D.—reported by Salzer et al. (2013) and was necessary to obtain the most accurate measure of physiological limits on bristlecone and foxtail pine growth at these sites. According to Salzer et al. (2013), today's climate is about 1.5 °C warmer than during the period of treeline stabilization implying treeline position in the Great Basin may be out of equilibrium with the current climate. There is documented evidence of seedling establishment in these areas up to 200m above current treeline positions, indicating a potential shift up-slope in treeline position may be underway (Salzer et al. 2013; Millar et al. 2015).

Treelines have long been recognized for their value as a indicator of large-scale climatic change. Great Basin bristlecone pine treeline chronologies—and to a lesser extent foxtail pine treeline chronologies from the southern Sierra Nevada—are especially important paleoclimatic indicators due to their extremely long lifespan, and researchers' ability to reconstruct environmental variables from annually resolved ring widths. Work by Bunn et al. (2011) demonstrates the importance of building chronologies from trees with a single, common limiting factor, to display the clearest climatic signal. This necessitates that chronologies include samples limited by a common environmental variable when building paleoclimatic reconstructions. Salzer et al. (2014) report a threshold 60m - 80m below treeline, above which bristlecone pine ring widths correlate positively with growing season temperatures, and below which they do not. The possibility that current treeline position in the Great Basin may be lower than the climatic conditions permit (see Appendix II) implies a potential change in the growth-limiting factor at and directly below treeline at these sites. Salzer et al. (2014) demonstrate this effect, reporting a divergence between tree growth and temperature on southern aspects in the White Mountains, CA, very close to SHP. The topoclimate models presented in this analysis indicate that temperatures on southern aspects at SHP are typically warmer than other aspects (at the same elevation), inferring it may only be a matter of time until similar effects are seen on other aspects.

Further, this analysis allows for future study of historic treelines at these sites. On the landscape there exist standing dead snags and remnant wood well above current tree positions, at MWA, SHP, and CSL. By dating remnant samples against the established chronologies, estimates of historic treeline positions have been calculated at these sites (Salzer et al. 2014), and front range of the Colorado Rocky Mountains (Carrara and McGeehin 2015). Validation of these estimates may now be possible with the classification models from this analysis, using using adjusted climate data to represent the climatic conditions during the period of interest. Additionally, this technique could enable a calculation of how far specific samples were from treeline position for a given time period, providing inference about the most-limiting environmental factor based on the sample's proximity to treeline. This would allow for specific samples to be removed from a chronology for a given period if their proximity to treeline indicated a different limiting factor targeted by the chronology.

5 Conclusions

This study analyzes the influence of topography on 1 meter temperatures in mountainous environments in the Great Basin, and the ability of specific climatic variables can predict specific bristlecone and foxtail pine treeline positions. I present four site-specific data sets consisting of five climatic variables at monthly-resolution, modeled from topographic data, that show the extent to which specific topographic characteristics influence each climate variable. I use these mapped variable layers to predict the treeline position at three of the four study locations. The results of this study, while comparable to other treeline analyses, are specific to the locations and species used in this analysis, and caution must be exercised when applying the conclusions of this study to other locations and species.

The results indicate: (1) topographic effects on 1 meter temperatures in mountainous environments in the Great Basin are measurable, and account for much of the variance not explained by elevation; (2) there are physiological limits related to summer temperatures and growing season characteristics on bristlecone and foxtail pine growth, resulting in treeline formation; (3) these limits are perhaps best represented by a calculation of growing degree

hours above 5 °C and/or average monthly temperature; (4) bristlecone and foxtail pine treeline position in Great Basin may be predicted exclusively from climate and topography data, and share a similar isotherm to the average of treelines globally.

6 Appendix I: PRISM and iButton Comparisons

Presented here are plots displaying the iButton average of daily temperatures recorded at each site and obtained from the PRISM model (PRISM 2004), as referenced in section 2.3.2. These plots show the stable relationship between PRISM and the iButton values, allowing for the missing days temperatures to be modeled from the PRISM data.

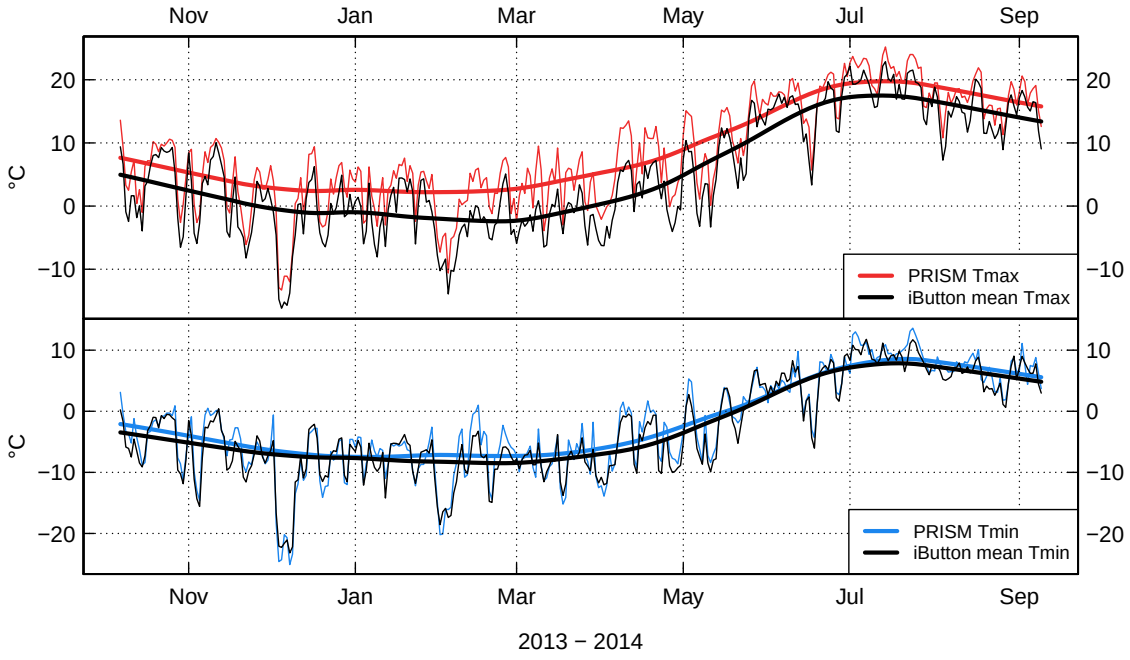

Figure 13: MWA comparisons between daily PRISM values and iButton averages. Top plot shows maximum temperatures, bottom shows minimum temperatures.

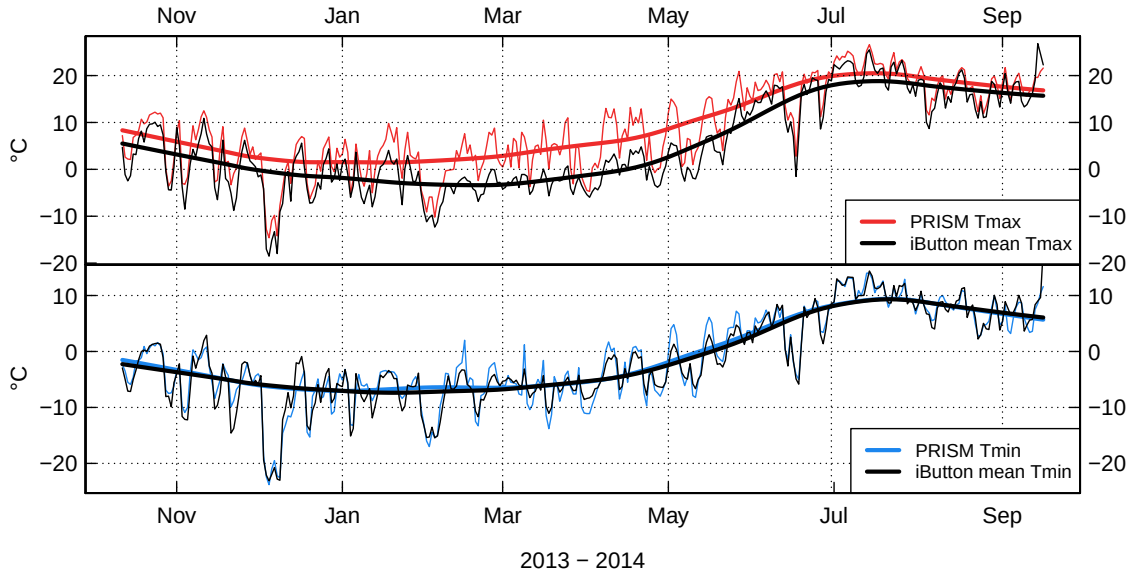

Figure 14: PRL comparisons between daily PRISM values and iButton averages. Top plot shows maximum temperatures, bottom shows minimum temperatures.

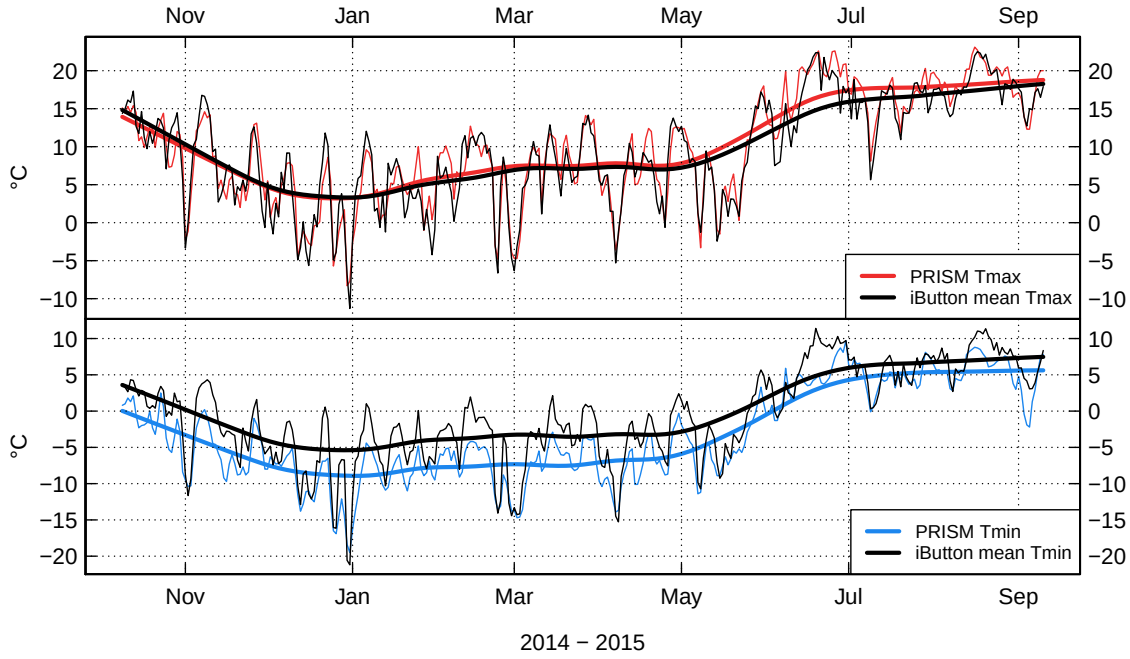

Figure 15: CSL comparisons between daily PRISM values and iButton averages. Top plot shows maximum temperatures, bottom shows minimum temperatures.

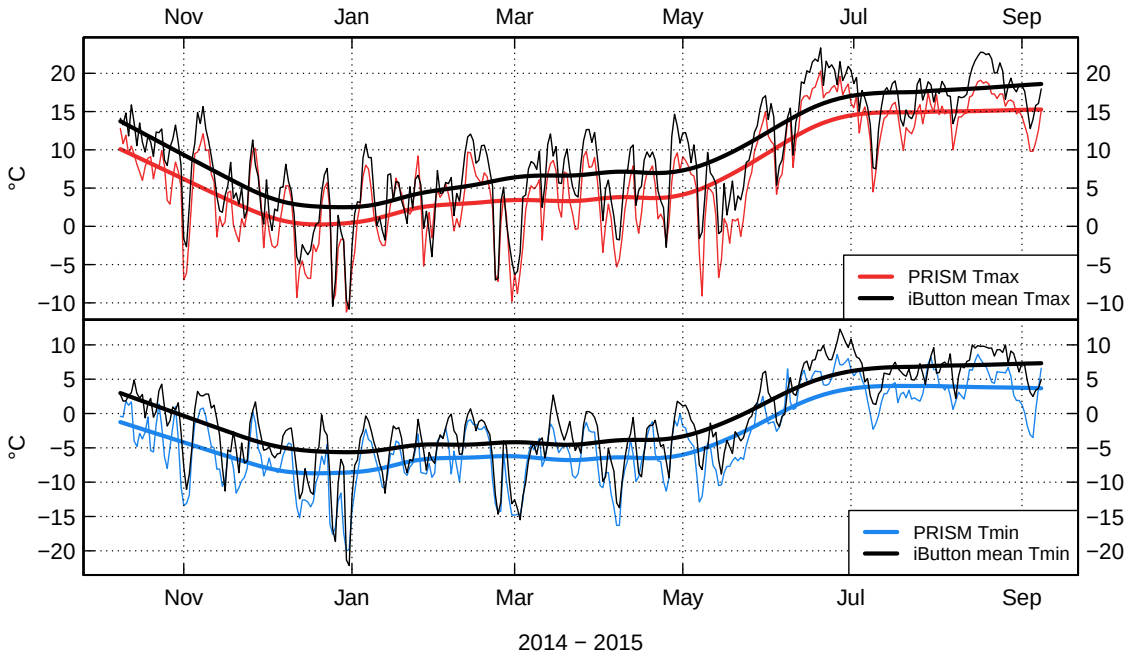

Figure 16: SHP comparisons between daily PRISM values and iButton averages. Top plot shows maximum temperatures, bottom shows minimum temperatures.

7 Appendix II: Potential Treeline Position Projections

Figures 10 to 12 predict treeline position as a function of the climate during the period of treeline position stabilization. Using inputs that are representative of the climate during the 20th century, I used the same models to project the *potential* treeline position based on the current climate, and determined an estimate of the climate sensitivity of these treelines. The projections are first-order approximations of how treelines at my might respond to recent climatic change, plainly speaking there is a high level of uncertainty associated with each projection and extreme caution should be used when drawing conclusions from this data. These projections are very sensitive to changes in climatic conditions, indicating each model may be over fit slightly to its location. The global theory for climate limited treelines proposes a common mechanism for treeline formation, and because the models have different parameters and structures, they are likely over fit to varying degrees. Thus seemingly small changes to the inputs may have amplified affects on the final treeline potential projection, as seen in figures 17 to 19.

Another assumption is that there is no seasonality in the delta calculation of 1.5 °C used in the paleoclimate adjustment. While the average climate may have warmed by a 1.5 °C since the early 1300s, this value may not be constant across all seasons. If so, the importance of monthly predictors in the classification models may be different. Herein lies the benefit of the LGS and SMT variables for treeline prediction, as changes in seasonality may not alter the predictive power of these variables as much as individual monthly topoclimate variables. These physiological variables are representative of the entire growing season, so while the length and average temperature may change, the predictive value may not be as affected as much as specific months due to differences in warming throughout the year. This being said, these projections are my best estimate for potential treeline position given the data available and the methodology of this analysis.

(Körner 2012) states treeline position shifts lag changes in climate by *at least* 50-100 years, and is heavily coupled to the relatively slow demographic processes of recruitment and establishment. Other studies indicate fluctuations in the Great Basin treeline position operate

on even longer timescales (100's of years) (Scuderi 1987; Salzer et al. 2013). It follows that specific climatic events, or short periods (relative to the suggested lag period) of anomalous weather conditions will not act to influence treeline position (Lloyd and Graumlich 1997). Thus, it is unknown (a) how long current conditions must persist to initiate an upslope migration of treeline, and (b) how quickly treeline position would move once an upward trend has started.

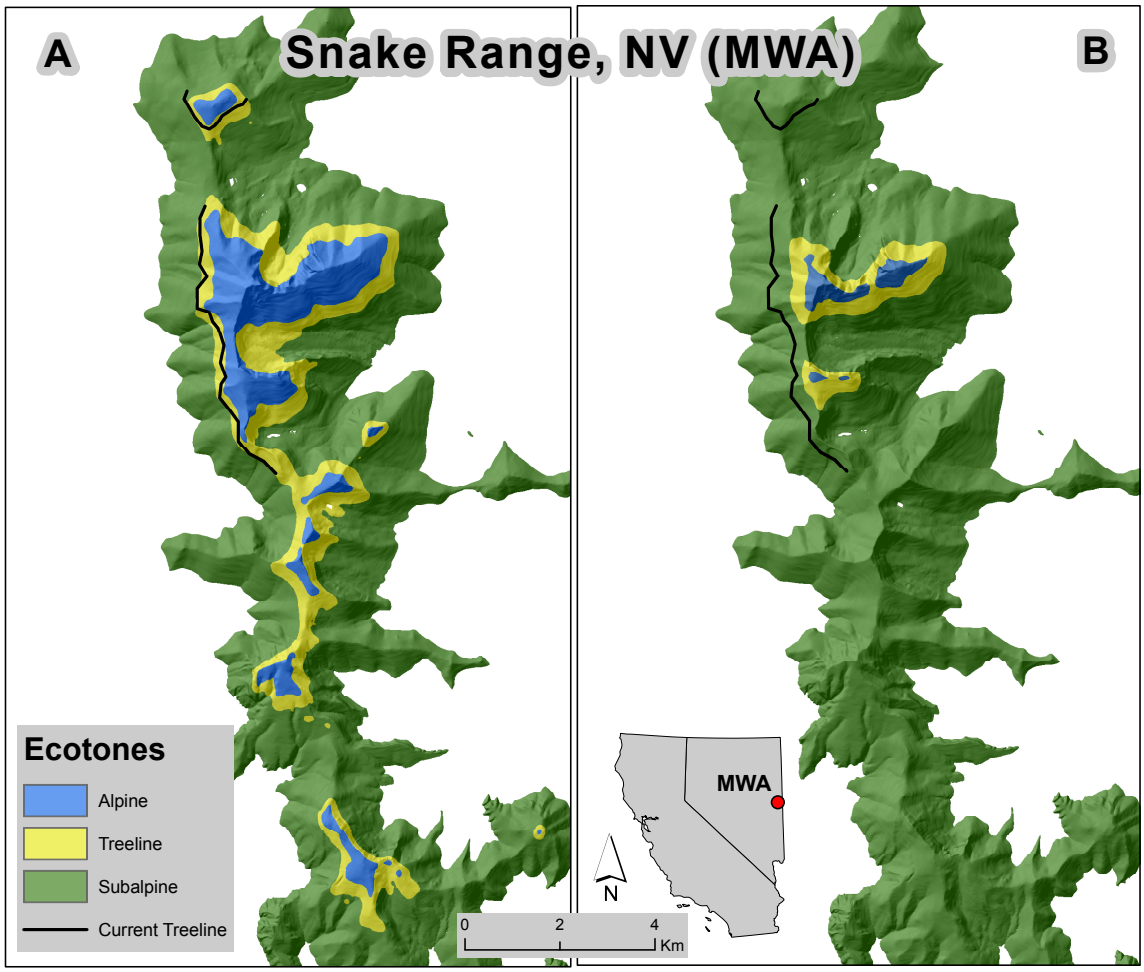

Figure 17: Smoothed ecotone projections in the Snake Mountain Range, NV, showing current treeline position (**A**) and potential treeline position based on recent global warming (**B**). The black line represents the treeline areas used to build the model. These areas were chosen because of their obvious climate limitation, with no indications of recent, non-climate related disturbance. **A** MWA treeline model projections of current treeline position, using climate inputs representative of the climate during treeline position formation. This projection is the best prediction of the spatial distribution of the ecotones available given these methods. **B** Ecotone projections for the current climate based on a constant 1.5 °C of warming applied to all monthly climate variables. There is a significant decrease in the amount of alpine and treeline ecotone, indicating a possible combination of extreme sensitivity in this model to changing climatic conditions, and its tendency to be over fit to this location.

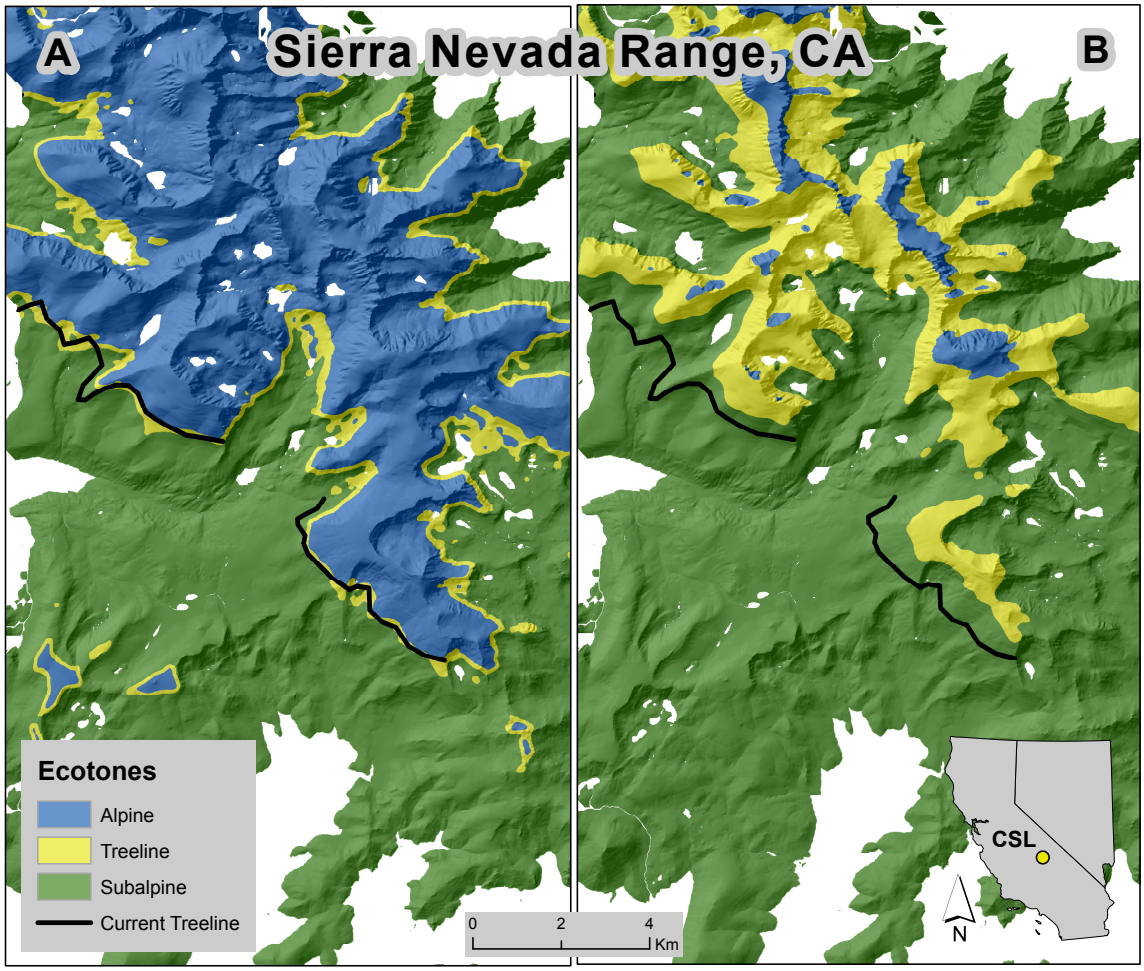

Figure 18: Smoothed ecotone projections in the Sierra Nevada, CA, showing current treeline position (**A**) and potential treeline position based on recent global warming (**B**). The black line represents the treeline areas used to build the model. These areas were chosen because of their obvious climate limitation, with no indications of recent, non-climate related disturbance. **A** CSL treeline model projections of current treeline position, using climate inputs representative of the climate during treeline position formation. This projection is the best prediction of the spatial distribution of the ecotones available given these methods. **B** Ecotone projections for the current climate based on a constant 1.5 °C of warming applied to all monthly climate variables. There is a significant decrease in the amount of alpine ecotone, indicating a possible combination of extreme sensitivity in this model to changing climatic conditions, and its tendency to be over fit to this location. Additionally, this projection is interesting in that it predicts the treeline ecotone to grow in area, even as it migrates upslope. This seems contradictory to other research regarding the future of treeline ecotones (Körner 2012; Paulsen and Körner 2014) and is worth further investigation.

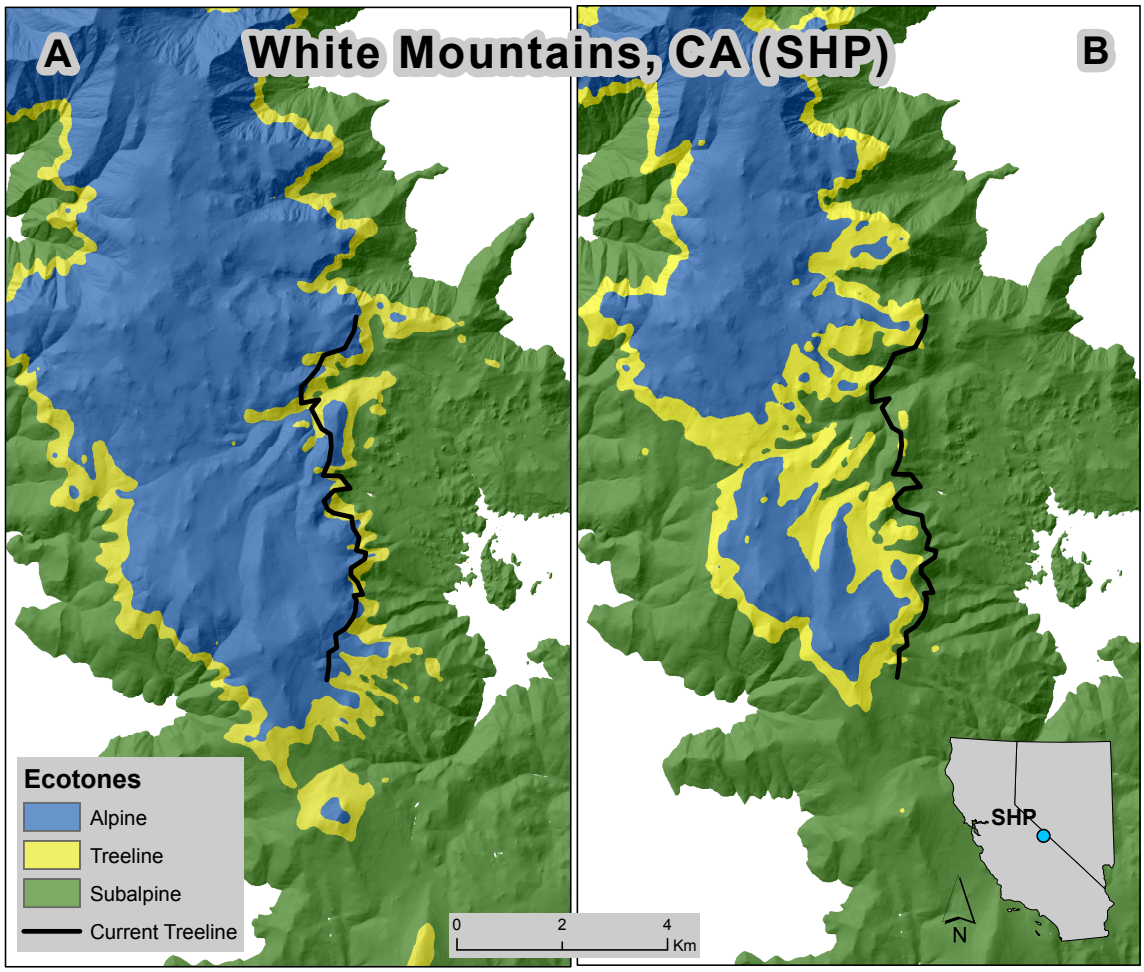

Figure 19: Smoothed ecotone projections in the White Mountains, CA, showing current treeline position (**A**) and potential treeline position based on recent global warming (**B**). The black line represents the treeline areas used to build the model. This area was chosen because of its obvious climate limitation, with no indications of recent, non-climate related disturbance. **A** SHP treeline model projections of current treeline position, using climate inputs representative of the climate during treeline position formation. This projection is the best prediction of the spatial distribution of the ecotones available given these methods. **B** Ecotone projections for the current climate based on a constant 1.5 °C of warming applied to all monthly climate variables. There is a significant decrease in the amount of alpine and treeline ecotone, indicating a possible combination of extreme sensitivity in this model to changing climatic conditions, and its tendency to be over fit to this location. Interestingly this site has the least upslope migration (measured horizontally) of treeline position, which may be due to a steeper average slope at this site.

References

Adams, H. R., H. R. Barnard, and A. K. Loomis. 2014. Topography alters tree growth–climate relationships in a semi-arid forested catchment. *Ecosphere*, 5(11):pp. 1–16.

Ashcroft, M. B., L. A. Chisholm, and K. O. French. 2009. Climate change at the landscape scale: predicting fine-grained spatial heterogeneity in warming and potential refugia for vegetation. *Global Change Biology*, 15(3):pp. 656–667.

Breiman, L., J. Friedman, C. J. Stone, and R. A. Olshen. 1984. *Classification and regression trees*. CRC press.

Bunn, A. G., M. K. Hughes, and M. W. Salzer. 2011. Topographically modified tree-ring chronologies as a potential means to improve paleoclimate inference. *Climatic Change*, 105(3):pp. 627–634.

Carrara, P. E. and J. P. McGeehin. 2015. Evidence of a higher late-Holocene treeline along the Continental Divide in central Colorado. *The Holocene*, 25(11):pp. 1829–1837.

Chung, U. and J. I. Yun. 2004. Solar irradiance-corrected spatial interpolation of hourly temperature in complex terrain. *Agricultural and forest meteorology*, 126(1):pp. 129–139.

Currey, D. R. 1965. An ancient bristlecone pine stand in eastern Nevada. *Ecology*, pp. 564–566.

Dobrowski, S. Z. 2011. A climatic basis for microrefugia: the influence of terrain on climate. *Global change biology*, 17(2):pp. 1022–1035.

Dobrowski, S. Z., J. T. Abatzoglou, J. A. Greenberg, and S. Schladow. 2009. How much influence does landscape-scale physiography have on air temperature in a mountain environment? *Agricultural and Forest Meteorology*, 149(10):pp. 1751–1758.

ESRI. 2012. Arcgis desktop. release 10.1.

Fridley, J. D. 2009. Downscaling climate over complex terrain: high finescale (¡ 1000 m) spatial variation of near-ground temperatures in a Montane forested landscape (Great Smoky Mountains). *Journal of Applied Meteorology and Climatology*, 48(5):pp. 1033–1049.

Fritts, H. 1976. *Tree rings and climate*. Academic Press.

Geiger, R., R. H. Aron, and P. Todhunter. 2009. *The climate near the ground*. Rowman & Littlefield.

Hughes, M. K. and G. Funkhouser. 2003. Frequency-Dependent Climate Signal in Upper and Lower Forest Border Tree Rings in the Mountains of the Great Basin. *Climatic Change*, 59(1):pp. 233–244.

Jobbagy, E. G. and R. B. Jackson. 2000. Global controls of forest line elevation in the northern and southern hemispheres. *Global Ecology and Biogeography*, 9(3):pp. 253–268.

Kipfmueller, K. F. and M. W. Salzer. 2010. Linear trend and climate response of five-needle pines in the western United States related to treeline proximity. *Canadian journal of forest research*, 40(1):pp. 134–142.

Körner, C. 2007. Climatic treelines: conventions, global patterns, causes (klimatische baumgrenzen: konventionen, globale muster, ursachen). *Erdkunde*, 61(4):pp. 316–324.

Körner, C. 2008. Winter crop growth at low temperature may hold the answer for alpine treeline formation. *Plant Ecology & Diversity*, 1(1):pp. 3–11.

Körner, C. 2012. *Alpine treelines: functional ecology of the global high elevation tree limits*. Springer Science & Business Media.

Körner, C. and J. Paulsen. 2004. A world-wide study of high altitude treeline temperatures. *Journal of Biogeography*, 31(5):pp. 713–732.

Kuhn, M. 2015. *caret: Classification and Regression Training*. R package version 6.0-47.

LaMarche Jr, V. C. 1973. Holocene climatic variations inferred from treeline fluctuations in the White Mountains, California. *Quaternary Research*, 3(4):pp. 632–660.

LaMarche Jr, V. C. 1974a. Frequency-dependent relationships between tree-ring series along an ecological gradient and some dendroclimatic implications. *Tree-Ring Bulletin*.

LaMarche Jr, V. C. 1974b. Paleoclimatic inferences from long tree-ring records intersite comparison shows climatic anomalies that may be linked to features of the general circulation. *Science*, 183(4129):pp. 1043–1048.

LaMarche Jr, V. C. and C. W. Stockton. 1974. Chronologies from Termperature-Sensitive Bristlecone Pines at Upper Treeline in Western United States. *Tree-Ring Bulletin*.

Lloyd, A. H. and L. J. Graumlich. 1997. Holocene dynamics of treeline forests in the Sierra Nevada. *Ecology*, 78(4):pp. 1199–1210.

Lookingbill, T. R. and D. L. Urban. 2003. Spatial estimation of air temperature differences for landscape-scale studies in montane environments. *Agricultural and Forest Meteorology*, 114(3):pp. 141–151.

Millar, C. I., R. D. Westfall, D. L. Delany, A. L. Flint, and L. E. Flint. 2015. Recruitment patterns and growth of high-elevation pines in response to climatic variability (1883–2013), in the western Great Basin, USA. *Canadian Journal of Forest Research*, 45(10):pp. 1299–1312.

Paulsen, J. and C. Körner. 2014. A climate-based model to predict potential treeline position around the globe. *Alpine Botany*, 124(1):pp. 1–12.

PRISM. 2004. Oregon state university.

Salzer, M. W., A. G. Bunn, N. E. Graham, and M. K. Hughes. 2013. Five millennia of paleotemperature from tree-rings in the Great Basin, USA. *Climate Dynamics*, 42(5-6):pp. 1517–1526.

Salzer, M. W., M. K. Hughes, A. G. Bunn, and K. F. Kipfmueller. 2009. Recent unprecedented tree-ring growth in bristlecone pine at the highest elevations and possible causes. *Proceedings of the National Academy of Sciences*, 106(48):pp. 20348–20353.

Salzer, M. W., E. R. Larson, A. G. Bunn, and M. K. Hughes. 2014. Changing climate response in near-treeline bristlecone pine with elevation and aspect. *Environmental Research Letters*, 9(11):p. 114007.

Scuderi, L. A. 1987. Late-Holocene upper timberline variation in the southern Sierra Nevada. *Nature*, 325(6101):pp. 242–244.

Sykes, M. T., I. C. Prentice, and W. Cramer. 1996. A bioclimatic model for the potential distributions of north European tree species under present and future climates. *Journal of Biogeography*, pp. 203–233.

Therneau, T., B. Atkinson, and B. Ripley. 2015. *rpart: Recursive Partitioning and Regression Trees*. R package version 4.1-9.

Wardle, P. 1971. An explanation for alpine timberline. *New Zealand journal of botany*, 9(3):pp. 371–402.

Weiss, A. 2001. Topographic position and landforms analysis. In *Poster presentation, ESRI User Conference, San Diego, CA*, pp. 200–200.

Weiss, D. J., G. P. Malanson, and S. J. Walsh. 2015. Multiscale relationships between alpine treeline elevation and hypothesized environmental controls in the western United States. *Annals of the Association of American Geographers*, 105(3):pp. 437–453.

Weiss, S. B., D. D. Murphy, and R. R. White. 1988. Sun, slope, and butterflies: topographic determinants of habitat quality for Euphydryas editha. *Ecology*, 69(5):pp. 1486–1496.

Wolock, D. M. and G. J. McCabe. 1995. Comparison of single and multiple flow direction algorithms for computing topographic parameters in topmodel. *Water Resources Research*, 31(5):pp. 1315–1324.